Vienna University of Technology

Master Thesis

An Implementation of Modal Pushover Analysis for Multistory Buildings in ANSYS

Author:
Bsc. Andra Valentina Kopandi

Supervisor:
Ao.Univ.Prof. Dipl.-Ing. Dr.techn.
Rudolf Heuer
Senior Scientist PhD Peter Rosko

A thesis submitted in fulfilment of the requirements for the degree of Master of Science

in the

Research Center of Mechanics and Structural Dynamics
E206 Institute of Building Construction and Technology

October 2014

Declaration of Authorship

I, Andra Valentina KOPANDI, declare that this thesis titled, 'An Implementation of Modal Pushover Analysis for Multistory Buildings in ANSYS' and the work presented in it are my own. I confirm that:

- This work was done wholly or mainly while in candidature for a research degree at this University.
- Where any part of this thesis has previously been submitted for a degree or any other qualification at this University or any other institution, this has been clearly stated.
- Where I have consulted the published work of others, this is always clearly attributed.
- Where I have quoted from the work of others, the source is always given. With the exception of such quotations, this thesis is entirely my own work.
- I have acknowledged all main sources of help.
- Where the thesis is based on work done by myself jointly with others, I have made clear exactly what was done by others and what I have contributed myself.

Signed: _____

Date: _____

"To see far is one thing, going there is another."

Constantin Brancuşi

VIENNA UNIVERSITY OF TECHNOLOGY

Abstract

Faculty of Civil Engineering
E206 Institute of Building Construction and Technology

Master of Science

An Implementation of Modal Pushover Analysis for Multistory Buildings in ANSYS

by Andra Valentina KOPANDI

Evaluated is the implementation of a modal pushover analysis for a multistory building in the finite element program ANSYS. In this analysis method the seismic demand of the inelastic system is determined by a pushover analysis using the inertia force distribution of each mode. The total estimate is obtained by combining the results of the respective modal demands. Finally these results are compared with results obtained by nonlinear response history analysis and with results from other scientific studies. The thesis is structured as follows: the theory of the modal pushover analysis and the implementation for a nonlinear system in ANSYS is discussed in the first two chapters. Subsequently a 9 story building from the SAC project is chosen and described for the implementation of the nonlinear problem. In the last chapters, the results are evaluated and a conclusion is drawn.

Acknowledgements

I would like to express my deep gratitude to Ao.Univ.Prof. Dipl.-Ing. Dr.techn. Rudolf Heuer and Senior Scientist PhD Peter Rosko, my research supervisors, for their patient guidance, enthusiastic encouragement and useful critiques of this research work. I also wish to thank my family and friends for their support and encouragement throughout my study.

Contents

List of Figures

List of Tables

Abbreviations

POA	**P**ush**o**ver **A**nalysis
MPA	**M**odal **P**ushover **A**nalysis
SDOF	**S**ingle **D**egree **o**f **F**reedom
MDOF	**M**ulti **D**egree **o**f **F**reedom
CSM	**C**apacity **S**pectrum **M**ethod
ESDOF	**E**quivalent **S**ingle **D**egree **o**f **F**reedom
FEMA	**F**ederal **E**mergency **M**anagement **A**gency
SAC	**S**EAOC **A**TC **C**UREE
SEAOC	**S**tructural **E**ngineers **A**ssociation **o**f **C**alifornia
ATC	**A**pplied **T**echnology **C**ouncil
MRF	**M**oment **R**esisting **F**rame
RHA	**R**esponse **H**istory **A**nalysis

Symbols

$[M]$	mass matrix of MDOF system
$[C]$	damping matrix of MDOF system
$[Q]$	storey force vector of MDOF system
$\{\phi\}$	mode shape vector
$\{1\}$	influence vector
$\ddot{x_g}$	ground acceleration history
x_t	roof/top displacement of MDOF
$\dot{x_t}$	relative velocity of roof
$\ddot{x_t}$	relative acceleration of roof
x^*	reference displacement of ESDOF system
$\dot{x}^*$	reference velocity of ESDOF system
$\ddot{x}^*$	reference acceleration of ESDOF system
$[M]^*$	mass of ESDOF system
$[C]^*$	damping of ESDOF system
$[Q]^*$	force relationship of ESDOF system
$\dot{x}^*$	reference velocity of ESDOF system
$\ddot{x}^*$	reference acceleration of ESDOF system
V_b	base shear of MDOF system
V_y	yield strength of MDOF system
K_e	effective elastic stiffness of MDOF system
K_S	hardening/softening stiffness
α	strain-hardening ratio
x_y	yield displacement of MDOF system
x_y^*	yield displacement of ESDOF system
$[Q]_y^*$	yield force of ESDOF system

i	storey number
j	mode number
T_{eq}	elastic period of ESDOF system
F_i	applied force at ith storey
W_i	weight of ith storey
ϕ_{ij}	ith storey element of the mode shape vector for mode j
h_i	height of the ith storey
n	total number of modes, total number of storeys
$S_d(T_n)$	acceleration ordinate of the design spectrum at period T_n
T_n	fundamental period of vibration
C_{vx}	vertical distribution factor
k	coefficient dependent on the fundamental period T_n
a_{mr}	modification factor in Kunnath load pattern
Γ_j	participation factor for mode j
φ_{ij}	mass-normalised mode shape of ith storey for jth mode
$S_a(\varsigma_j, T_j)$	spectral acceleration for a given earthquake
M_i	mass of the ith-storey
S_a	spectral acceleration of inelastic ESDOF
S_d	spectral displacement of inelastic ESDOF
α_m	modal mass coefficient
M	total mass of structure
a_{pi}	initial performance acceleration of ESDOF for CSM method
d_{pi}	initial performance point of ESDOF for CSM method
β_{eq}	equivalent viscous damping of inelastic ESDOF system
β_0	equivalent viscous damping due to hysteresis
S_{ae}	pseudo-acceleration ordinate from the response spectrum
S_{de}	elastic displacement ordinate from the response spectrum
μ	ductility factor
R_μ	strength reduction factor
S_n^*	modal force distribution
r_n	peak modal response
u_{rn}	roof displacement at mode n
V_{bn}	base shear at mode n

u_{rny}	roof displacement at yield point
V_{bny}	base shear at yield point
M_n^*	effective modal mass
D_n	deformation response of the nth-"mode" inelastic SDF system
D_{ny}	deformation response at yield point
ϕ_n	nth natural vibration mode of the structure
ϕ_{rn}	value of ϕ_n at the roof

Chapter 1

Theory

1.1 Performance Based Design

1.1.1 General

During the last 40 years the sector of Earthquake Engineering has advanced considerably due to the rapid developments of computers and computing, the improved experimental facilities, and the development of new methods of seismic design and assessment of structures. This development has led to an improvement of the named design procedures with a shift from traditional force-based procedures to displacement-based procedures. The characterization of the various performance levels has led to performance-based earthquake engineering.

The practice of performance based engineering arose from the realization that buildings had to be designed to explicitly ensure life safety, not necessarily attempting to reduce damage in a structure. Thus buildings should be constructed based on their intended use, to meet the performance objectives indicated in figure 1.1. In the figure, each combination of an earthquake return period and performance level represents a specific design performance objective. The intent is that ordinary buildings provide life safety for any earthquake; and that for frequent earthquakes, the building user not be burdened with extensive repairs or loss of use; that buildings required for emergency response and essential public function should not be damaged beyond a level that would permit their

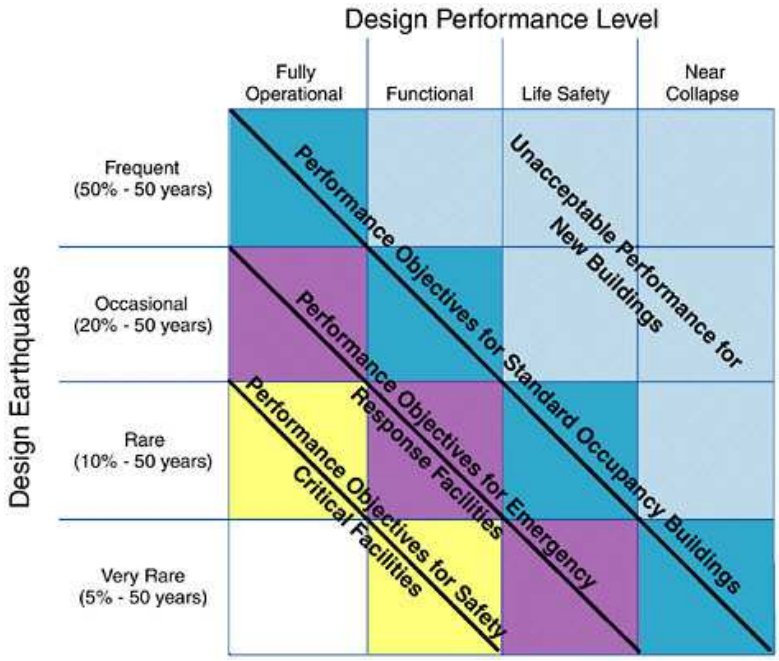

FIGURE 1.1: Performance Objectives [9]

use, and; that facilities housing systems and materials that would pose a hazard to many persons if released, have a low risk of damage resulting in such release [9].

The earthquake performance of buildings describes the damage incurred to the building's structure, envelope, partitions, ceilings, mechanical/electrical systems, and contents. While the building performance is a continuum, for design purposes it is convenient to identify discrete performance levels for the major structural and other building components that significantly affect building function, property protection, and safety [1]. Standards [2] generally provide guidance on three performance levels:

- Immediate Occupancy, IO: Achieve essentially elastic behavior by limiting structural damage. Structure substantially retains original strength and stiffness and there is no permanent drift. Minor cracking of facades, partitions, and ceilings as well as structural elements can occur. All systems important to normal operation are functional.

- Life Safety, LS: Limit damage of structural and nonstructural components so as to minimize the risk of injury or casualties and to keep essential circulation routes accessible. Life Safety, means the post-earthquake damage state in which significant damage to the structure has occurred, but some margin against either partial

or total structural collapse remains. It should be possible to repair the structure; however, for economic reasons this may not be practical.

- Collapse Prevention, CP: means the building is near collapse. However, all significant components of the gravityload-resisting system must continue to carry their gravity load demands. Significant risk of injury may exist.

1.1.2 Demand Parameters-Acceptance Criteria

Once these objectives are defined, the next step is to identify specific demand parameters and appropriate acceptance criteria in order to quantitatively evaluate the performance levels.

The performance acceptance criteria may be specified for the overall systems, substructures, or components of a building. They may also vary with the type of analysis employed (for instance static or dynamic nonlinear analysis) and also with the way uncertainties are handled.

In the next step the structure must be modeled and analyzed in order to calculate the values of the demand parameters. The demand parameters typically include peak forces and deformations in structural and nonstructural components, story drifts, and floor accelerations and provide insights into the overall building response and damage to nonstructural components. Other demand parameters, such as cumulative deformations or dissipated energy, may be checked to help confirm the accuracy of the analysis and/or to assess cumulative damage effects.

The performance is checked by comparing values of demand parameters (short: "demands") to the acceptance criteria ("capacities") for the desired performance level. Thus the capacity, the ability of the building to resist seismic loads must be greater than the demands, the earthquake effects on the building. The comparison often occurs through "demand-capacity" ratios.

1.1.3 Procedures for Earthquake Analysis

There are four analytical procedures for design and assessment purposes recommended in the guidelines [10, 11]. These are the Linear Static Procedure, LSP, Linear Dynamic

Procedure, LDP, Nonlinear Static Procedure, NSP, and the Nonlinear Dynamic Procedure, NDP, with ascending order of complexity.

A. Linear Static Procedure:

Under Linear Static Procedure, design seismic forces and the corresponding internal forces and displacements are determined using a linearly elastic, static analysis. A pseudo lateral load is applied to the building in order to approximate the maximum displacement which is to be expected during the design earthquake. If the building responds essentially elastically to the design earthquake, the calculated internal forces will be reasonable approximations of those expected during the design earthquake. However this will often not be the case. The results of the linear procedures can be very inaccurate when applied to buildings with highly irregular structural systems, vertical mass or stiffness irregularity or buildings exceeding a certain Height, as well as structures with elements that have large ductility demands or the lateral force resisting system is non-orthogonal. Thus restrictions on the applicability of this procedure must be carefully checked.

B. Linear Dynamic Procedure:

Under the Linear Dynamic Procedure forces and displacements are determined using a linearly elastic, dynamic analysis. The response calculations are carried out using either modal spectral analysis or Time-History Analysis. Modal spectral analysis is carried out using linearly-elastic response spectra that are not modified to account for anticipated nonlinear response. Modal responses are combined using rational methods to estimate total building response quantities. As with the LSP, it is expected that the LDP will produce displacements that are approximately correct, but will produce internal forces that exceed those that would be obtained in a yielding building.

C. Nonlinear Static Procedure:

In the nonlinear static procedure, the structural model is subjected to an incremental lateral load whose distribution represents the inertia forces expected during ground shaking. The lateral load is applied until the imposed displacements reach the so-called "target displacement," which represents the displacement demand that the earthquake ground motions would impose on the structure. Once loaded to the target displacement, the demand parameters for the structural components are compared with the respective acceptance criteria for the desired performance state. The NSP should not be used unless

comprehensive knowledge of the structure has been obtained. In the case of slender, tall buildings, higher mode effects must be taken into account.

D. Nonlinear Dynamic Analysis Procedure:

The nonlinear dynamic procedure, when properly implemented, provides a more accurate calculation of the structural response to strong ground shaking. Since the nonlinear dynamic analysis model incorporates inelastic member behavior under cyclic earthquake ground motions, the nonlinear dynamic procedure explicitly simulates hysteretic energy dissipation in the nonlinear range. The dynamic response is calculated for input earthquake ground motions, resulting in response history data on the pertinent demand parameters. This analysis involves fewer assumptions than the nonlinear static procedure and so is subject to fewer limitations than nonlinear static procedure. However, as this accurate analysis involves the implementation of a complex analytical model as well as a high computational effort, many prefer the usage of Nonlinear Static Procedure.

1.1.4 Evaluation of the methods

Clearly the nonlinear dynamic procedure that predicts the forces and cumulative deformations (damage) demands in every element of the structural system is the most accurate solution. However, the implementation of this solution requires the availability of a set of ground motion records that account for the uncertainties and differences of the possible earthquake characteristics. It requires further the capability to model adequately the cyclic load-deformation characteristics of all important elements of the soil-foundation structure system, as well as the knowledge of element deformation capacities.

It is stated that there is a need to work on this final solution but also a need to recognize the time and financial constraints imposed on engineering offices as well as the limitation of today's states of knowledge and practice [12]. Even in those situations where the expertise and resources for running time-history analyses are available, it is often the case that preliminary simpler analysis (i.e. modal and static analyses) are run to enable a first check of the model. Errors in the definition/assemblage of a finite elements model are difficult to detect from dynamic analysis results, while in the case of a pushover analysis they tend to be relatively evident.

In this context, the goal is to perform an analysis that is relatively simple and captures the essential features of the system. The accuracy of demand prediction is desirable, but may not be essential, since neither seismic input nor capacities are known with accuracy. The inelastic static analysis (pushover analysis) serves this purpose provided enough knowledge of its implementation and limitations is available [13].

1.2 Pushover Analysis

1.2.1 Purpose

The purpose of the Pushover Analysis is to evaluate the performance of a structural system by estimating its strength and deformation demands in design earthquake and comparing these demands to available capacities at the performance levels of interest [13]. Important performance parameters are: global drift, interstory drift, inelastic element deformations and element and connection forces. The pushover analysis can be viewed as a method of predicting force and deformation demands, which accounts for the redistribution of internal forces when the structure is deformed beyond its elastic range.

The pushover analysis is expected to provide response characteristics that cannot be obtained from an elastic static or dynamic analysis such as:

- The realistic force demands on potentially brittle elements
- Verification of the adequacy of load path
- Estimates of deformation demands for elements that have to deform inelastically in order to dissipate energy
- Identification of strength discontinuities in plan and elevation
- Identification of the critical regions in which the deformation demands are expected to be high

1.2.2 Basic Steps

A model directly incorporating inelastic material response is displaced to a target displacement, and resulting internal deformations and forces are determined. The mathematical model of the building is subjected to monotonically increasing lateral forces or displacements until either a target displacement is exceeded or the building collapses. The target displacements represents the maximum displacement likely to be experienced during the design earthquake. Because the mathematical model accounts for several types of nonlinearity, the calculated internal forces will be reasonable approximations of those expected during the design earthquake. Results of the analysis are checked using applicable acceptance criteria. Calculated displacements and internal forces are compared directly with allowable values.

The majority of the Nonlinear Static procedures follow the same basic steps:
1. A pushover analysis is performed. A lateral load pattern is applied and the base shear- roof displacement curve, also called the pushover curve is plotted.
2. The pushover curve is idealized and an equivalent Single Degree of Freedom System, ESDOFS, based on the pushover curve is defined.
3. The target displacement is estimated, according to a selected design response spectrum.
4. The SDOFS response and the actual response of the structure are related by means of a shape coefficient, typically identified in the first mode participation factor.
5. Finally, the response parameters, storey drift and forces on each structural member, can be evaluated, knowing the global demand, through the pushover curve (or capacity curve) of the system.

1.2.3 Theoretical Background

The accuracy of NSA is mainly based on three assumptions:
1) the load pattern used in performing pushover analyses, that influences the shape of the capacity curve as well as the distribution of seismic demand along the height of the

structure;

2) the procedure to derive the idealized equivalent SDOF from the pushover curve;

3) the estimation of the target displacement.

Those assumptions will be further discussed.

1.2.3.1 Control Node Displacement

The Location of the control node, assumed as the global displacement parameter, is at the center of mass at the roof of the building. The displacement of the node is calculated for the specified loads and afterwards compared with the target displacement — a displacement that characterizes the effects of earthquake shaking.

1.2.3.2 Lateral Load Pattern

The Lateral Load Pattern applied to the MDOF System is critical for the performance evaluation and has been recognized that it affects the results significantly. The load patterns are intended to represent the distribution of inertia forces in a design earthquake. This distribution will vary during a severe earthquake but usually the assumption that the forces will be reasonably constant throughout the earthquake leads to the usage of a constant lateral load pattern. In order to capture the response of a dynamic system it has been agreed that at least two load patterns should be applied to the system [10, 11].

1. The uniform load pattern is usually the first load pattern to be used and it is based on lateral forces that are proportional to the total mass at each floor level. It emphasizes the demands on lower stories compared to the demands in upper stories as well as story shear forces compared to overturning moments.

$$F_i = W_i \tag{1.1}$$

Where W_i is the effective seismic weight of the 'i' story, including dead loads.

2. The Lateral load pattern proportional to story inertia forces is calculated by combination of modal responses using (1) Response Spectrum Analysis of the building including a sufficient number of modes to capture 90 Percent of the total mass, and (2) the appropriate ground motion spectrum.

$$F_i = W_i \phi_{ij} \tag{1.2}$$

Where ϕ_{ij} is the ith element of the mode shape vector corresponding to the 'i' storey for mode j.

3. Inverted triangular distribution may also be used.

$$F_i = \frac{W_i h_i}{\sum_{i=1}^{n} W_i h_i} V_b \tag{1.3}$$

where h_i is the height of the 'i' story, n is the total number of the stories, and Vb is the base shear given by the following equation:

$$V_b = S_d(T_n) W \tag{1.4}$$

where $S_d(T_n)$ is the acceleration ordinate of the design spectrum at the fundamental period T_n, and W is the total weight of the structure.

4. The FEMA 356 load distribution which may be used if more than 75 Percent of the total mass participates in the fundamental mode in the direction under consideration;

$$F_x = C_{vx} V \tag{1.5}$$

$$C_{vx} = \frac{W_x h_x^k}{\sum_{i=1}^{n} W_i h_i^k} \tag{1.6}$$

Where C_{vx} is the vertical distribution factor, h_i height from base to floor level i, h_x height from base to floor level x and V is the pseudo lateral load, calculated through the coefficient method.

5. Kunnath's Load distribution

$$F_i = \sum_{j=1}^{n} a_{mr} \Gamma_j M_i \varphi_{ij} S_a(\varsigma_j, T_j) \tag{1.7}$$

where a_{mr} is a modification factor that can control the relative effects of each included mode and which can take positive or negative values; usually positive or negative unity, Γ_j is the participation factor for mode j, M_i is the mass of the ith-storey, φ_{ij} is the mode shape of the ith-storey for mode j, $S_a(\varsigma_j, T_j)$ is the spectral acceleration for a given earthquake loading at frequency corresponding to the period T and damping ratio ς for mode j.

6. An adaptive load pattern utilizing an elastic demand spectrum. In this procedure, equivalent seismic loads are calculated at each pushover step using the instantaneous mode shapes. The corresponding elastic spectral accelerations are used for scaling of the lateral loads which are applied to the structure in each mode independently. While these adaptive force distributions may provide better estimates of seismic demands, they are conceptually complicated and computationally demanding for routine application in structural engineering practice.

The implementation of several load patterns is related to the different types of pushover analysis which will be discussed in the following chapter. After applying the forces, a nonlinear incremental static analysis of the MDOF structure can be carried out from which it is possible to determine the force-deformation characteristics of the ESDOF system. The outcome of the analysis of the MDOF structure is a Base Shear, V_b, - Roof Displacement, U_t, diagram, the global force-displacement curve or capacity curve of the structure. This capacity curve provides valuable information about the response of the structure because it approximates how it will behave after exceeding its elastic limit.

1.2.3.3 Idealization of the pushover curve

The static pushover analysis has no robust theoretical background. It is based on the assumption that the response of the multi-degree-of-freedom (MDOF) structure is directly related to the response of an equivalent single-degree-of-freedom (ESDOF) system with appropriate hysteretic characteristics. The deflected shape of the MDOF system can be represented by a shape vector ϕ that remains constant throughout the time history, regardless of the level of deformation.

Defining the relative displacement vector X of an MDOF system as (roof displacement), the governing differential equation of an MDOF system can be written as

$$[M]\{\phi\}\ddot{x_t} + [C]\{\phi\}\dot{x_t} + [Q] = -[M]\{1\}\ddot{x_g} \tag{1.8}$$

where [M] is the mass matrix, [C] is the damping matrix, [Q] is the story force vector, $\{1\}$ is an influence vector characterising the displacements of the masses when a unit ground displacement is statically applied, and $\ddot{x_g}$ is the ground acceleration.

We define the reference SDOF displacement x^* as

$$x^* = \frac{\{\phi\}^T[M]\{\phi\}}{\{\phi\}^T[M]\{1\}}x_t \tag{1.9}$$

and pre-multiply equation (1.8) by ϕ^T, and substitute for x_t using equation (1.9). We obtain the following differential equation for the response of the equivalent SDOF system:

$$[M]^*\ddot{x}^* + [C]^*\dot{x}^* + [Q^*] = -[M]^*\ddot{x_g} \tag{1.10}$$

[M]*, [C]* and [Q]* denote the properties of the equivalent SDOF system and are given by

$$[M]^* = \{\phi\}^T[M]\{1\} \tag{1.11}$$

$$[Q]^* = \{\phi\}^T[Q] \tag{1.12}$$

$$[C]^* = \{\phi\}^T[C]\{\phi\}\frac{\{\phi\}^T[M]\{1\}}{\{\phi\}^T[M]\{\phi\}} \tag{1.13}$$

The multilinear pushover curve of the MDOF Structure is idealized by a bilinear relationship that defines a 'yield' strength, V_y, an effective 'elastic' stiffness, $K_e = V_y/\delta_{t,y}$, and a hardening (or softening) stiffness, $K_S = \alpha K_e$ for the structure. The simplified bilinear base shear-roof displacement response curve, is needed to define the properties of the equivalent SDOF system.

The yield value of the base shear V_y and the corresponding roof displacement $X_{t,y}$ are used together with equations (1.9) and (1.12) to compute the force - displacement relationship for the equivalent SDOF system:

$$x_y^* = \frac{\{\phi\}^T[M]\{\phi\}}{\{\phi\}^T[M]\{1\}} x_{t,y} \tag{1.14}$$

$$[Q]_y^* = \{\phi\}^T[Q]_y \tag{1.15}$$

where Q_y is the story force vector at yield, i.e. $V_y = \{1\}^T Q_y$. The initial period of the equivalent SDOF system T_{eq} can be computed as:

$$T_{eq} = 2\pi \left[\frac{x_y^* M^*}{Q_y^*}\right]^{\frac{1}{2}} \tag{1.16}$$

The strain hardening ratio α of the MDOF structure defines the strain hardening ratio of the equivalent SDOF system. Thus the basic properties of the equivalent SDOF system are known.

1.2.3.4 The Target Displacement

The target displacement of pushover analysis should approximate the maximum level of deformation that is expected during the design earthquake. It can be calculated by any procedure that accounts for the effects of non-linear response on displacement amplitude. The properties of the equivalent SDOF system, together with spectral information for inelastic SDOF system, provide the information necessary to estimate the target displacement. A convenient definition of target displacement is the roof displacement at the center of mass of the structure. There are several ways to determine the target displacement, which will be discussed later in this thesis.

1.2.4 Pushover Analysis Methods

There are three different general groups of pushover Analysis: the Conventional POA methods, the Adaptive POA methods, and the Energy-Based POA methods. The Conventional POA methods are the following:

1. Capacity Spectrum Method , CSM
2. Improved Capacity Spectrum Method, ICSM
3. N2 method
4. Displacement Coefficient Method, DCM
5. Modal Pushover Analysis, MPA

The Capacity Spectrum Method, the N2 Method and the Modal Pushover Analysis will be further discussed. The Adaptive and Energy-Based POA are more recent sophisticated variations of the Conventional POAs and will not be presented.

1.2.4.1 The Capacity Spectrum Method

In the CSM the base shear forces and roof displacements calculated through pushover analysis are converted to equivalent spectral accelerations and spectral displacements, respectively, by means of coefficients that represent effective modal masses and modal participation factors. These spectral values define the capacity spectrum. The demands of the earthquake ground motion are represented by response spectra. The performance of the structure is then estimated by including both capacity and demand spectra in a graphical construction and intersecting the two curves.

The procedure can be summarized by the following steps:

1.Lateral loads are applied to the MDOF System based to the fundamental mode of vibration. Other lateral loads may as well be used. The Pushover Curve in terms of roof displacement x_t vs. Base shear V_b is plotted.

2. The capacity curve is idealized as a bilinear relationship with the choice of a global yield point (V_y, u_y) of the structural system and a final displacement (V_{pi}, u_{pi}). The areas above and under the curve are approximately equal in order to ensure that there is equal energy associated with each curve.

The conversion of the MDOF system to the ESDOF System and its dynamic characteristics are calculated as previously described.

3. By use of dynamic characteristics, the X_t vs. V_b capacity curve is converted to a S_a vs. S_d. capacity spectrum as follows:

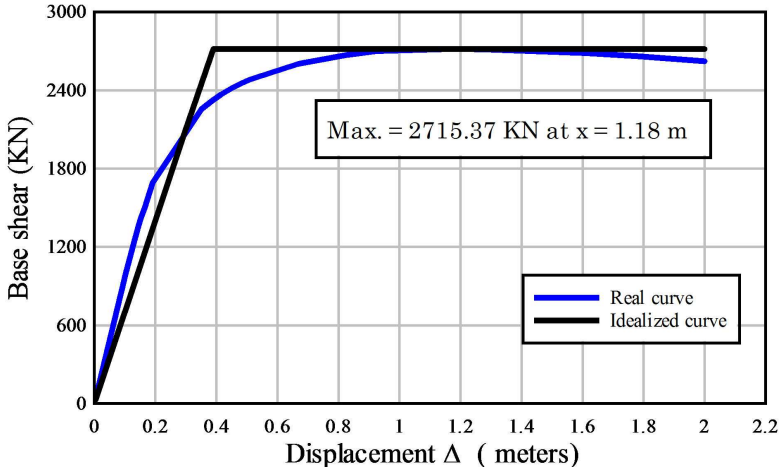

FIGURE 1.2: Example of an idealized capacity curve

$$S_a = \frac{V_b}{\alpha_m M} \tag{1.17}$$

$$S_d = \frac{u}{\Gamma_1 \phi_{ij}} \tag{1.18}$$

Where M is the total mass of the building, ϕ_{ij} is is the modal amplitude at storey level 'i' for mode j, Γ_1 is the participation factor and α_m is the modal mass coefficient, which are given by:

$$\Gamma_1 = \frac{\{\phi\}^T[M]\{1\}}{\{\phi\}^T[M]\{\phi\}} \tag{1.19}$$

$$\alpha_m = \frac{\left[\sum_{j=1}^{n} m_i \phi_{ij}\right]^2}{\sum_{i=1}^{n} m_i \sum_{j=1}^{n} m_i \phi_{ij}^2} \tag{1.20}$$

4.The response spectra is obtained for several levels of damping. The capacity spectrum and family of damped response spectra are plotted on an ADRS format (S_a vs S_d coordinates with period T lines radiating from origin).

5. The intersection of the capacity spectrum with the appropriately damped response spectrum represents an initial estimate of the performance point (a_{pi}, d_{pi}). The intersection between the two curves can be based on the equal displacement rule or other

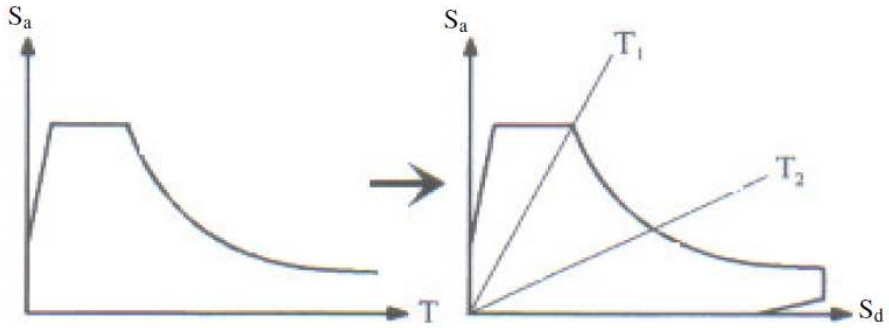

FIGURE 1.3: Conversion to ADRS Format

rules.

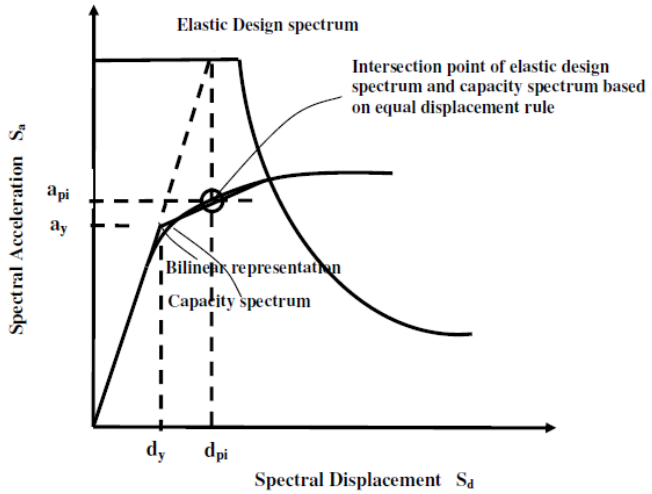

FIGURE 1.4: Initial performance point estimation

6. Equivalent viscous damping of the spectrum is estimated based on the specific maximum displacement d_{pi}. A new response spectrum has to be computed for the calculated amount of damping.

$$\beta_{eq} = \beta_0 + 0.05 \tag{1.21}$$

7. The new demand spectrum should then be checked if it intersects the capacity spectrum at or close enough to the estimate of performance point. If the demand spectrum intersects the capacity spectrum within an acceptable tolerance then the estimate is accepted. Otherwise the performance point is re-estimated and the procedure is repeated.

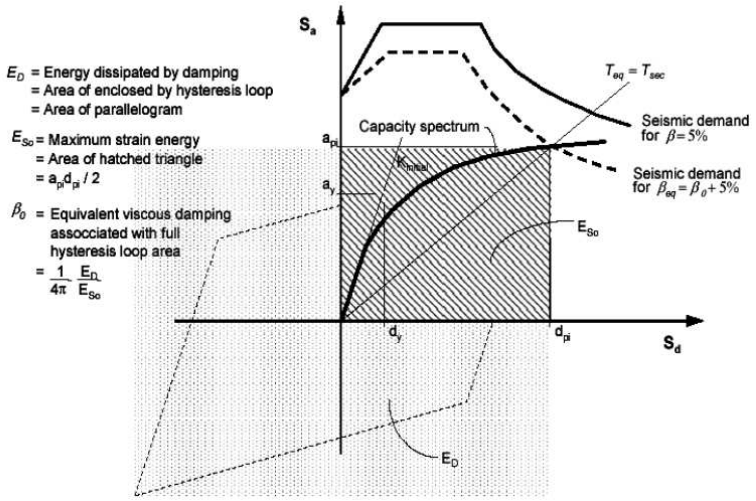

FIGURE 1.5: Equivalent viscous damping estimation [2]

1.2.4.2 The N2 Pushover Procedure

The N2 procedure was developed at the University of Ljubljana in Slovenia in mid-eighties. It is a novelty in EC8. The method is based on the following steps:

1.Compute the lateral force pattern. In the N2 method, the vector of the lateral load F used in the pushover analysis is given by:

$$F = P[M]\{\phi\} \tag{1.22}$$

where P controls the lateral load magnitude, [M] is the mass matrix and ϕ is the mode shape vector.

The pushover analysis should be performed using both of the following lateral load patterns (EC8 4.3.3.4.2.2):

A uniform load pattern: which yields in $\phi_i = 1$,and the lateral forces becomes:

$$F = \frac{F_i}{\sum_{j=1}^{n} m_j} F_b = \frac{F_i}{\sum_{j=1}^{n} m_j} P \tag{1.23}$$

where Fb is the base shear force and m_i and m_j are the storey masses.

A modal pattern: which can be:

a. Inverted triangular pattern or

b. A pattern that simulates the peak inertia forces of the fundamental mode shape. The lateral forces become:

$$F = \frac{m_i \phi_i}{\sum_{j=1}^{n} m_j \phi_i} F_b \tag{1.24}$$

2. Perform the pushover analysis. This step is the same as for the Capacity Spectrum Method and as previously described.

3.Compute the equivalent SDOF capacity curve. The pushover curve is converted to a Capacity Spectrum relationship for the equivalent SDOF system using the following equations:

$$S_a = \frac{V_b}{\Gamma_j M^*} \tag{1.25}$$

$$S_d = \frac{u}{\Gamma_j \phi_n} \tag{1.26}$$

where $M^* = \sum M_i \phi_{ij}$ is the effective mass of the building, ϕ_n is the roof element of the mode shape vector, and Γ_j is the participation factor for mode j. The capacity spectrum is then plotted in the ADRS format.

4.Idealize the capacity curve as an elastic-perfectly plastic. An approximate bilinear idealisation of the capacity spectrum is performed in order to determine the yield strength F_y^* , yield displacement u_y^* from the bilinear capacity curve and effective period T_{eq} of the ESDOF system as described for the CSM Method.

5. Compute the seismic demand according to EC8. For an elastic SDOF system, the following relationship applies:

$$S_{de} = \frac{T^2}{4\pi^2} S_{ae} \tag{1.27}$$

where S_{ae} and S_{de} are the values on the elastic acceleration and displacement spectrum respectively, corresponding to the period T and a fixed viscous damping. For an inelastic

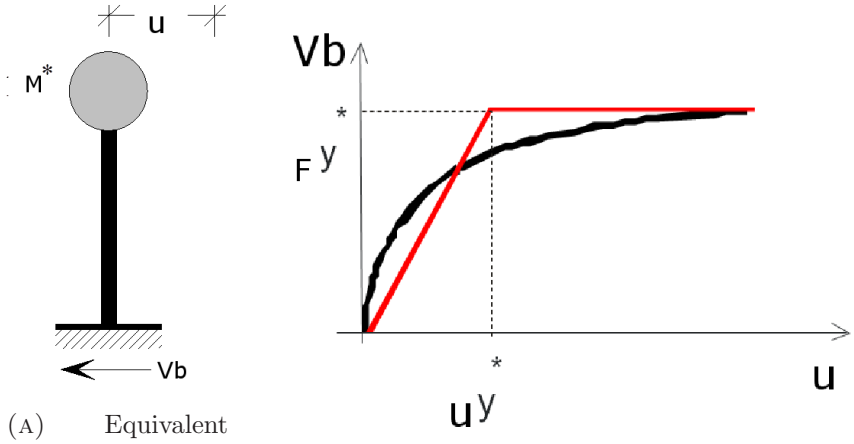

(A) Equivalent SDOF

(B) Idealization of the pushover curve

spectrum, the acceleration S_a and the displacement S_d can be determined as:

$$S_a = \frac{S_{ae}}{R_\mu} \tag{1.28}$$

$$S_d = \frac{\mu}{R_\mu} S_{de} \tag{1.29}$$

where μ is the ductility factor, defined as the ratio between ultimate displacement and the yield displacement of the SDOF system. R_μ is the reduction factor due to ductility:

$$R_\mu = \begin{cases} (\mu - 1)\dfrac{T}{T_c} + 1 & \text{if } T < T_c \quad (1.30a) \\ \mu & \text{if } T \geq T_c \quad (1.30b) \end{cases}$$

6. Compute the target displacement of the MDOF system.

The structural response quantities to a given seismic load can not be extracted directly from the capacity curve of the pushover analysis. The target displacement must be estimated as the displacement demands for the corresponding equivalent SDOF system. According to EC8, the target displacement of the equivalent SDOF structure is determined from the 5 Percent damped elastic response spectrum. The displacement demand S_d of the ESDOF system can be determined by substituting eq. 1.30 into eq. 1.29. This leads to:

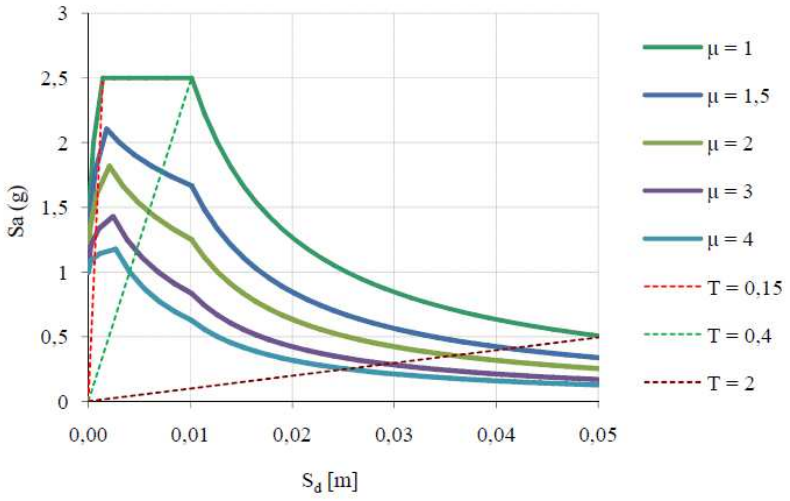

FIGURE 1.6: Demand spectra for constant ductility in AD format, normalized to 1,0g peak ground acceleration, for subsoil class A

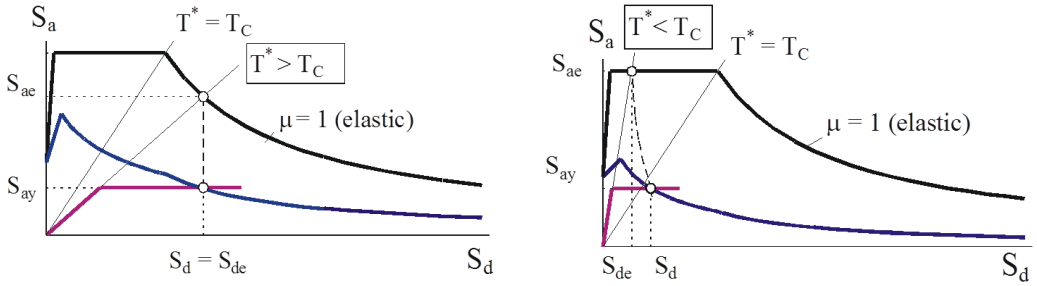

(A) Vibration period T^* longer than T_c (B) Vibration period T^* shorter than T_c

FIGURE 1.7: Computation of Target Displacement with the Equal Displacement Rule

$$S_d = \begin{cases} \dfrac{S_{de}}{R_\mu}\left((R_\mu - 1)\dfrac{T_c}{T} + 1\right) & \text{if } T < T_c \quad (1.31a) \\ S_{de} & \text{if } T \geq T_c \quad (1.31b) \end{cases}$$

Equation 1.31 implies that the displacement estimate will always be larger than the initial elastic displacement for short-period structures, or structures that have fundamental period lower than the characteristic period of the ground motion T_c. The elastic response spectra and demand spectra can be plotted as a spectral acceleration against spectral displacement, where the vibration period T^* is represented by radial lines. The above figure shows the determination of the target displacement of an equal SDOF system with (A) vibration period T^* longer than T_c and (B) period shorter than T_c.

1.2.4.3 Modal Pushover Analysis

Usually in a pushover analysis, it is assumed that the target displacement is controlled by a single shape vector- the first period of vibration. Parameter studies have shown that for frames and wall structures with a first mode period of less than 2 seconds this assumption is rather accurate for elastic systems and conservative (overestimates the MDOF displacement) for inelastic systems. This assumption though doesn't account for higher mode effects which are to be expected in a tall structure, buildings with more than 6 storys in general, which result in a first mode period larger than 2 seconds. Anil K. Chopra and Rakesh K. Goel have devoloped the Modal Pushover Analysis, which includes the contributions of several modes of vibration of the building.

Summarized below are the steps necessary for estimating the peak response of a building using the modal analysis procedure:

1. Compute the natural frequencies, ω_n and modes, ϕ_n, for linearly elastic vibration of the building

2. For the nth-mode, develop the base shear-roof displacement, $V_{bn} - u_n$, pushover curve for force distribution

$$S_n^* = m\phi_n \tag{1.32}$$

where m is the mass matrix of the structure. The structure pushed to the roof displacement, u_{rno} the peak value of the roof displacement due to the nth-mode:

$$u_{rno} = \Gamma_n \phi_{rn} D_n \tag{1.33}$$

where $D_n = A_n/\omega_n^2$. D_n or A_n are readily available from the response (or design) spectrum.

3. Idealize the pushover curve as a bilinear curve. If the pushover curve exhibits negative postyielding stiffness, idealize the pushover curve as elastic-perfectly-plastic.

4. Convert the $V_{bn} - u_{rn}$ idealized pushover curve to the $F_{sn}/L_n - D_n$ relation for the nth -"mode" inelastic SDF system. The two sets of forces and displacements are related

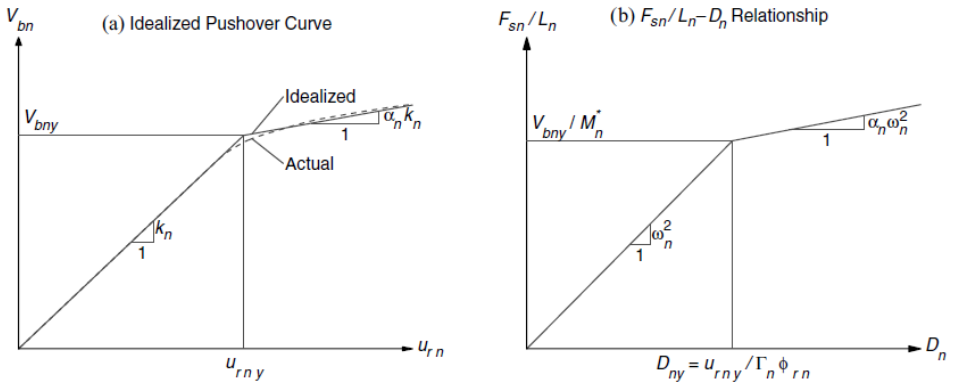

FIGURE 1.8: Properties of the nth-'mode' inelastic SDF system from the pushover curve [6]

as follows:

$$F_{sn} = \frac{V_{bn}}{\Gamma_n} \tag{1.34}$$

$$D_n = \frac{u_{rn}}{\Gamma_n \phi_{rn}} \tag{1.35}$$

Equations 1.34 and 1.35 enable conversion of the pushover curve to the desired F_{sn}/L_n–D_n relation shown in Figure 1.8, where the yield values of F_{sn}/L_n and D_n are

$$\frac{F_{sny}}{L_n} = \frac{V_{bny}}{M_n^*} \tag{1.36}$$

$$D_{ny} = \frac{u_{rny}}{\Gamma_n \phi_{rn}} \tag{1.37}$$

in which V_{bny} and u_{rny} are the base shear and roof displacement at the yield point, $M_n^* = L_n\Gamma_n$ is the effective modal mass, ϕ_{rn} is the value of ϕ_n at the roof, and $\Gamma_n = \phi_n^T m_1/\phi_n^T m\phi_n$.

5. Compute peak deformation D_n of the nth-"mode" inelastic SDOF system defined by the force deformation relation and damping ratio ς_n. The elastic vibration period of the system is

$$T_n = 2\pi \left(\frac{L_n D_{ny}}{F_{sny}}\right)^{1/2} \tag{1.38}$$

For an SDF system with known Tn and ς_n , D_n can can be computed by nonlinear response history analysis (RHA) or from the inelastic design spectrum.

6. Calculate peak roof displacement urn associated with the nth-"mode" inelastic SDF system from

$$u_{rn} = \Gamma_n \phi_{rn} D_n \tag{1.39}$$

7. From the pushover database (Step 2), extract values of desired responses r_n: floor displacements, story drifts, plastic hinge rotations, etc.

8. Repeat Steps 3-7 for as many modes as required for sufficient accuracy. Typically, the first two or three "modes" will suffice.

9. The peak 'modal' responses r_n, each determined by one pushover analysis, is combined using an appropriate modal combination rule, to obtain an estimate of the peak value r of the total response. This application of modal combination rules to inelastic systems lacks a theoretical basis. However, it provides results for elastic buildings that are identical to the well-known RSA procedure. The SRSS rule can be used:

$$r = \left(\sum_n r_n^2 \right)^{1/2} \tag{1.40}$$

1.2.5 Limitations of Pushover Analysis and Conclusion

As previously described, the pushover analysis is a very useful tool for estimating the deformation demands of a building. While the simplicity of the method makes it a more attractive approach for everyday practice than nonlinear time-history analysis, the method exhibits significant shortcomings and limitations, which are summarised below:

1. The theoretical background of the method is not rigorous, being based on the assumption that the MDOF response is related to the response of a SDOF oscillator. The pushover analysis is generally based on a series of assumptions and therefore, in-depth knowledge of the problem is needed in order to yield meaningful results.

2. The response of the MDOF system is highly dependent on the pattern of the applied lateral force. Higher mode effects have to be taken into account, especially for buildings

with more than 5 storys. Thus more than one load pattern has to be applied to the structure and results have to be compared.

3. It is difficult to model three-dimensional and torsional effects. Pushover analysis is very well established and has been extensively used with 2-D models. Extensive study and the implementation of the method to asymmetric 3-D systems, with stiffness or mass irregularities, still need to be carried out.

4. The progressive stiffness degradation that occurs during the cyclic non-linear earthquake loading of the structure is not taken into account. This degradation leads to changes in the periods and the modal characteristics of the structure. This affects the loading of the structure during an earthquake and would lead to a difference in the applied load patterns.

5. Being a static method, pushover analysis concentrates on the strain energy of the structure. Other sources of energy dissipation, which are associated with the dynamic response, are neglected, such as the kinetic and the viscous damping energy. Moreover, it does not take into account duration effects and cumulative energy dissipation demand.

6. The procedure mostly provides a convenient and fairly reliable method for structures whose dynamic response is governed by first-mode sway motions. In general, it will yield good results for low-rise buildings (less than about five stories) with symmetrical regular floor plan and elevation.

None of the invariant force distributions can account for the contributions of higher modes to response, or for a redistribution of inertia forces because of structural yielding and the associated changes in the vibration properties of the structure. (chopra) Several researchers have proposed adaptive force distributions, yet they are conceptually complicated and computationally demanding for routine application in structural engineering practice. Given this issues, attempts have been made to improve the static pushover analsysis while retaining the conceptual simplicity and computational attractiveness of the procedure with invariant force distribution. A. K. Chopra and R. K. Goel proposed the Modal Pushover Analysis, which has been previously described, which employs more than one modal distribution of the forces. It will be further used to investigate the response of a 9-story building. The finite element program Ansys will be employed in order to generate the pushover curve, which describes the nonlinear response of the

building and is essential in the pushover analysis. In the next Chapter the use of the finite element program for resolving complex nonlinear problems will be described.

Chapter 2

Implementation of Nonlinear Problems in ANSYS

2.1 General Modeling Techniques

2.1.1 Nonlinear Demand Parameters

As mentioned in the previous chapter, the performance of a building is checked by comparing the calculated values of demand parameters to the acceptance criteria for the desired performance level.

Structural components can be divided into two distinct groups: deformation - controlled and strength controlled components, depending on how ductile the reaction of each component is. In case of real structures, most components exhibit a certain degree of inelastic behaviour. Nevertheless, the distinction provides a guideline for modeling the structure and for establishing requirements. Deformation-controlled components must be modeled as inelastic, whereas force-controlled components can be simplified as being elastic. Demand parameters are deformation and strength, as well as velocities, accelerations, story drifts that provide overall building response and damage.

2.1.2 Structural Analysis Model Types

Inelastic structural component models can be differentiated by the way that plasticity is distributed through the member cross sections and along its length. Numerous models have been proposed in engineering literature for inelastic analysis of steel structures. In general, these models may be categorized into two main types: (1) Plastic zone (also called distributed plasticity); and (2) plastic hinge (also called concentrated plastic hinge)[14].

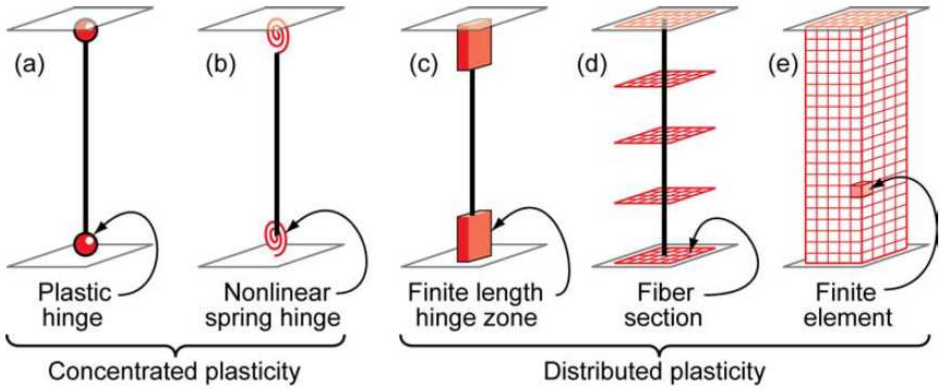

FIGURE 2.1: Idealized models of beam-column elements [1]

A. Concentrated Plasticity

The simplest models concentrate the inelastic deformations at the end of the element, such as through a rigid-plastic hinge (Figure 2.1, a) or an inelastic spring with hysteretic properties (Figure 2.1, b). By concentrating the plasticity in zero-length hinges with moment-rotation model parameters, these elements have relatively condensed numerically efficient formulations. Regions in the members other than at the plastic hinges are assumed to behave elastically. For slender structures in which elastic instability is the predominant mode of failure, both the elastic-plastic hinge and plastic-zone methods lead to almost identical results. However, for structures that exhibit significant yielding in the members, the elastic-plastic hinge method often overpredicts the actual stiffness and strength of the structure.

B. Distributed Plasticity

The plastic-zone approach follows explicitly the gradual spread of yielding throughout the volume of the structure. Plastification in the members is modeled by discretization of members into several beam-column elements and subdivision of the cross sections

into many fibers. Because of the refined discretization of the members and their cross sections, the plastic-zone analysis can predict accurately the inelastic response of the structure and is generally considered an exact method of analysis.

- The finite length hinge model (Figure 2.1, c) is an efficient distributed plasticity formulation with designated hinge zones at the member ends. Cross sections in the inelastic hinge zones are characterized through either nonlinear moment-curvature relationships or explicit fiber-section integrations that enforce the assumption that plane sections remain plane. The inelastic hinge length may be fixed or variable, as determined from the moment-curvature characteristics of the section together with the concurrent moment gradient and axial force. Integration of deformations along the hinge length captures the spread of yielding more realistically than the concentrated hinges, while the finite hinge length facilitates calculation of hinge rotations.

- The fiber formulation (Figure 2.1, d) models distribute plasticity by numerical integrations through the member cross sections and along the member length. Uniaxial material models are defined to capture the nonlinear hysteretic axial stress-strain characteristics in the cross sections. Uniaxial fibers are numerically integrated over the cross section to obtain stress resultants (axial force and moments) and incremental moment-curvature and axial force-strain relations. The cross section parameters are integrated numerically at discrete sections along the member length, using displacement or force interpolation.

- The most complex models discretize the continuum along the member length and through the cross section into finite elements with numerous input parameters. This type of modeling is the most complex but represents as well the most challenge in terms of computational effort. As with the fiber formulation, the strains calculated from the finite elements can be difficult to interpret relative to acceptance criteria that are typically reported in terms of hinge rotations and deformations.

Concentrated vs. Distributed Plasticity

Concentrated and finite length hinge models may consider the axial force-moment (P-M) interactions through yield surfaces. On the other hand, fiber and finite element models

capture the P-M response directly. While distributed plasticity formulations model variations of the stress and strain through the section and along the member in more detail, important local behaviors, such as strength degradation or the nonlinear interaction of flexural and shear, are difficult to capture without sophisticated models. On the other hand, concentrated hinge or spring models may capture better the nonlinear degrading response of members through adjustment using member test data on moment-rotations and hysteresis curves. While more sophisticated formulations may seem to offer better capabilities for modeling certain aspects of behavior, simplified models may capture more effectively the relevant feature with the same or lower approximation.

Cyclic Degradation

Degradation in strength and stiffness can occur under cyclic loading. It is usual to account for strength degradation in the "backbone" curves used for inelastic components. This then affects the shape of the push-over curve. ASCE 41 and EC8 provide guidelines for estimation of stiffness, strength, and deformation limits in steel, reinforced concrete, masonry and wood members. Shown in Figure 2.2 is an idealized force versus deformation relationship. The points represented in the curve include: effective yield (point B), peak strength (point C), residual strength (point D), and ultimate deformation (point E).

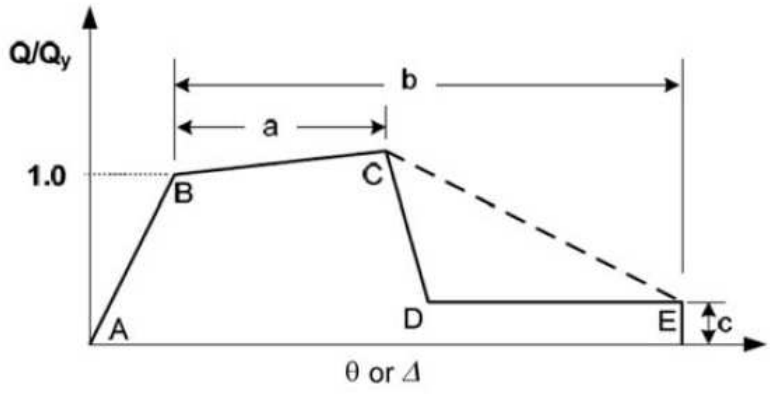

FIGURE 2.2: Generalized force-deformation curve. [2]

2.2 Structural Nonlinearities

2.2.1 Introduction

Many engineering problems can be solved using a linear approximation. In the Finite Element Analysis (FEA) the set of equations, describing the structural behaviour is then linear:

$$[K]\{D\} = \{F\}$$

In this matrix equation, [K] is the stiffness matrix of the structure, $\{D\}$ is the nodal displacements vector and $\{F\}$ is the external nodal force vector.

The Assumption underlying this equation are: displacements are small and can be neglected in equilibrium equations; the strain is proportional to the stress (linear Hookean material model), loads are conservative, independent on displacements, and supports of the structure remain unchanged.

If one of this approximations is abandoned, the problem becomes nonlinear. In Earthquake Engineering, where the structure is excited beyond its elastic range, implying large deformations, material yielding and nonlinear behavior of connection, this is usually the case. Thus the understanding of the nonlinear response is critical for performing a structural analysis for earthquake induced loads. The causes leading to nonlinear structural behavior have to be detected and taken into account. The set of equations becomes:

$$[K\ (D)]\{D\} = \{F\,(D)\}$$

The sources for nonlinearities can be grouped into three principal categories:

- Geometric Nonlinearity, also known as P-Delta Effect. If a structure experiences large deformations, its changing geometric configuration can cause the structure to respond nonlinearly. Geometric nonlinearity is characterized by "large" displacements and/or rotations. It is usually applied to slender structures, which are tipically steel structures as well as in stability porblmes of all types of problems.

- Material Nonlinearity: Nonlinear stress-strain relationships are a common cause of nonlinear structural behavior. The material behaviour depends on current deformation state as well as past history of the deformation. It may also depend on other variables such as temperature, creep, prestress etc.

- Nonlinear boundary conditions/nonlinear connections: it is common practice to treat boundary conditions and connections in steel structure as either perfectly rigid or pinned. In reality the behavior is semi-rigid with nonlinear moment-rotation response that influences the overall response of the structure.

These types of nonlinearities will be further discussed in this section.

Consequences of nonlinear structural behaviour that have to be recognized are:

- The principle of superposition cannot be applied. Thus, for example, the results of several load cases cannot be combined. Results of the nonlinear analysis cannot be scaled.

- Only one load case can be handled at a time.

- The sequence of application of loads (loading history) may be important. Especially, plastic deformations depend on a manner of loading. This is a reason for dividing loads into small increments in nonlinear FE analysis.

- The structural behaviour can be markedly non-proportional to the applied load.

- The initial state of stress (e.g. residual stresses from heat treatment, welding etc.) may be important. [15]

2.2.2 Solving the Nonlinear Equations

The equations of motion may be established from conservation of linear momentum. Substituting the FE approximations (and neglecting time dependent terms), the global equilibrium equations on discretized form is obtained:

$$\underbrace{\{R^{ext}\}}_{\text{externallyapplied loads}} = \underbrace{\{R^{int}\}}_{\text{nodal forces frominternal element stresses}}$$

$$\{R^{res}\} = \{R^{ext}\} - \{R^{int}\} = 0$$

where $\{R^{ext}\}$ and $\{R^{int}\}$ denote sum of externally applied loads and sum of internal element nodal forces, respectively.

$$\{R^{ext}\} = \sum_{i=1}^{N_{els}} \{r_e\}_i + \{P\} = \sum_{i=1}^{N_{els}} \left(\int_{V_i} [N]^T \{b\} dV + \int_{S_i} [N]^T \{t\} dS \right) + P$$

$$\{R^{int}\} = \sum_{i=1}^{N_{els}} \{r^{int}\}_i = \sum_{i=1}^{N_{els}} \left(\int_{V_i} [B]^T \{\sigma\} dV \right)$$

In order to satisfy equilibrium, external and internal forces have to be in balance. λ is a prescribed value of load or time parameter. The problem consists of finding the displacement vector $\{D\}$ which produces an internal force vector $\{R^{int}(D, \lambda)\}$ balancing externally applied loads $\{R^{ext}(\lambda)\}$. The fundamental equilibrium path (force-deformation relationship) has to be traced while traversing critical points (limit, turning and bifurcation points). A series of solutions have to be calculated: $\{D_n\}, \lambda_n$ for $n = 0, 1, 2, \ldots, n_{step}$ that within prescribed accuracy satisfy the equilibrium equation.

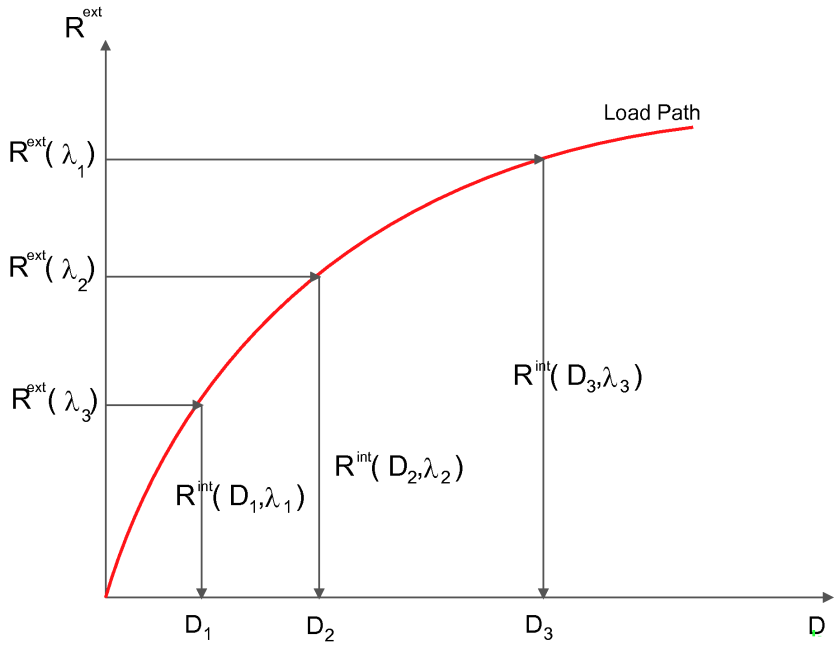

FIGURE 2.3: Solution Finding Process

By linearizing the residual of the global equilibrium equations the incremental form of the equations of motion expressed in terms of the incremental nodal displacements $\{\Delta D\}$ is obtained as:

$$\{R^{res}\}_{n+1}^{i+1} = \{R^{res}\}_{n+1}^{i} + \left[\frac{\partial R^{res}}{\partial D}\right]_{n+1}^{i} \{\Delta D\}_{n+1}^{i} = \{0\}$$

which results to:

$$[K_T]_{n+1}^{1} \{\Delta D\}_{n+1}^{i} = \{R^{res}\}_{n+1}^{i} \tag{2.1}$$

This is the incremental equation that advances the solution while satisfying the global equilibrium equations at each iteration 'i', within each time (load) step 'n+1', where

$$[K_T]_{n+1}^{1} = -\left[\frac{\partial R^{res}}{\partial D}\right]_{n+1}^{i} = \left[\frac{\partial R^{int}}{\partial D}\right]_{n+1}^{i} - \left[\frac{\partial R^{ext}}{\partial D}\right]_{n+1}^{i}$$

is the *tangent stiffness matrix*, which is also defined as:

$$[K_T] = [K_0] + [K_U] + [K_\sigma]$$

where $[K_0]$ is the linear stiffness matrix, $[K_U]$ is the initial displacement stiffness matrix and $[K_\sigma]$ is the initial stress stiffness matrix. The linear stiffness, which is independent on displacement, is familiar from small displacement structural analysis. The initial displacement stiffness reflects the effect of displacement on stiffness . The initial stress stiffness reflects the fact that there is an axial force in the bar prior to load increment.

Equation 2.1 is solved by subdividing the load in a series of load increments. Increments of ΔD are calculated and an updated solution is obtained as:

$$\{D\}_{n+1}^{i+1} = \{D\}_{n+1}^{i} + \{\Delta D\}_{n+1}^{i} \tag{2.2}$$

There are several methods to solve these simultaneous equations: the iterative Method, the Newton-Raphson method, the modified Newton-Raphson method and the Arch-Length Method.

2.2.3 Solving in ANSYS

In the past, costs associated with a nonlinear analysis prohibited its wider use. Today, rapid increases in computing power and concurrent advances in analysis methods made it possible to perform nonlinear analysis, taking into account the different types of nonlinearities and minimizing approximations.

The general-purpose Finite Element Analysis Program ANSYS, Inc. offers the necessary components for performing a nonlinear analysis: (a) element technologies for large-deformation treatment, (b) constitutive models for metals and nonmetals, (c) contact interaction and assembly analysis and (d) solution of large-scale problems (where multiple nonlinearities interact in a complex manner). One approach of solving nonlinear problems is, as stated before, to apply the load gradually by dividing it into a series of increments and adjusting the stiffness matrix at the end of each increment. The problem with this approach is that errors accumulate with each load increment, causing the final results to be out of equilibrium.

ANSYS employs the "Newton-Raphson" method to solve nonlinear problems. [16]

The Newton Raphson Iteration

Let $f(x)$ be a function and let r be a root of the equation $f(x) = 0$. The initial estimate of r is x_0, so that $r = x_0 + h$. The number $h = r - x_0$ measures how far the estimate x_0 is from the true root r. Since h is small, the linear (tangent line) approximation is used to conclude that

$$0 = f(r) = f(x_0 + h) \approx f(x_0) + hf'(x_0)$$

and therefore, unless $f'(x_0)$ is close to 0,

$$h \approx \frac{f(x_0)}{f'(x_0)} \quad and \tag{2.3}$$

$$r = x_0 + h \approx x_0 - \frac{f(x_0)}{f'(x_0)} \tag{2.4}$$

A new improved estimate x_1 of r is therefore given by

$$x_1 = x_0 - \frac{f(x_0)}{f'(x_0)}$$

Continuing in this way, if x_n is the current estimate, then the next estimate x_{n+1} is given by

$$x_{n+1} = x_n - \frac{f(x_n)}{f'(x_n)}$$

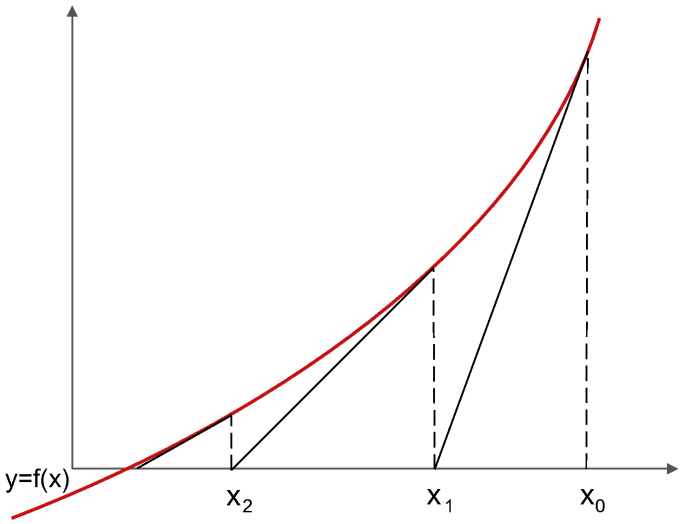

FIGURE 2.4: The Newton-Raphson Iteration

Implementation of the Method in ANSYS

ANSYS subdivides the load into a series of load increments. The load increments can be applied over several load steps. Figure 2.5 illustrates the use of Newton-Raphson equilibrium iterations in a single DOF nonlinear analysis.

Before each solution, the Newton-Raphson method evaluates the out-of-balance load vector, which is the difference between the restoring forces (the loads corresponding to the element stresses) and the applied loads. The program then performs a linear solution, using the out-of-balance loads, and checks for convergence. If convergence criteria are not satisfied, the out-of-balance load vector is re-evaluated, the stiffness matrix is updated, and a new solution is obtained. This iterative procedure continues until the problem converges. [16]

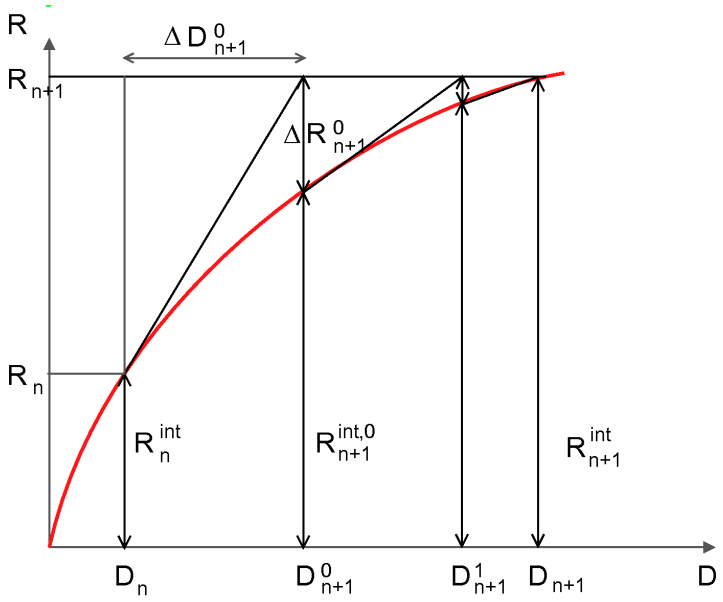

FIGURE 2.5: The Newton-Raphson Iteration in Ansys

A number of convergence-enhancement and recovery features, such as line search, automatic load stepping, and bisection, can be activated to help the problem to converge. By line searches (LS) an optimal incremental step length is obtained by minimizing the residual $\{R^{res}\}$ in the direction of $\{\Delta D\}$. LS can be particularly useful for problems involving rapid changes in tangent stiffness. If convergence cannot be achieved, then the program attempts to solve with a smaller load increment.

Newton's method is the most rapidly convergent process for solution of problems in which only one evaluation of the residual is made in each iteration. It can also achieve a very rapid convergence rate: it is the only method, provided that the initial solution is within the "ball of convergence", in which the asymptotic rate of convergence is quadratic. But there are several weaknesses of Newton's method:

- Computational expense: The tangent stiffness has to be computed and assembled at each iteration within each load step. If a direct solver is employed K_T also needs to be factored at each iteration within each load step.
- Increment size: If the time stepping algorithm used is not robust (self-adaptive), a certain degree of trial and error may be required to determine the appropriate load increments.

- Divergence: If the equilibrium path include critical points negative load increments must be prescribed to go beyond limit points. If the load increments are too large such that the solution falls outside "the ball of convergence" analysis may fail to converge.

Convergence Criteria

A convergence criteria measures how well the obtained solution satisfies equilibrium. In nonlinear finite element analysis the convergence criteria are usually based on some norm of the: Displacements (total or incremental), Residuals or Energy (product of residual and displacement). Although displacement based criteria seem to be the most natural choice they are not advisable in general as they can be misleadingly satisfied by a slow convergence rate. Residual based criteria are far more reliable as they check that equilibrium has been achieved within a specified tolerance in the current increment. Alternatively energy based criteria that use both displacements and residuals may be applied. However, energy criteria should not be used together with LS. In general nonlinear finite element analysis it is recommended that a combination of the three criteria is applied. The convergence criteria and tolerances must be carefully chosen so as to provide accurate yet economical solutions. If the convergence criterion is too loose inaccurate results are obtained. On the other hand, if the convergence criterion is too tight too much effort is spent in obtaining unnecessary accuracy.

Severe convergence difficulties are caused if the tangent stiffness matrix becomes singular (or non-unique). Such occurrences include nonlinear buckling analyses in which the structure either collapses completely or "snaps through" to another stable configuration as well as at limit, bifurcation or turning point in the load path. For such situations, an alternative iteration scheme can be activated, the arc-length method, to help avoid bifurcation points and track unloading.

The arc-length method

The arc-length method causes the Newton-Raphson equilibrium iterations to converge along an arc, thereby often preventing divergence, even when the slope of the load vs. deflection curve becomes zero or negative. This iteration method is represented schematically in Figure 2.6.

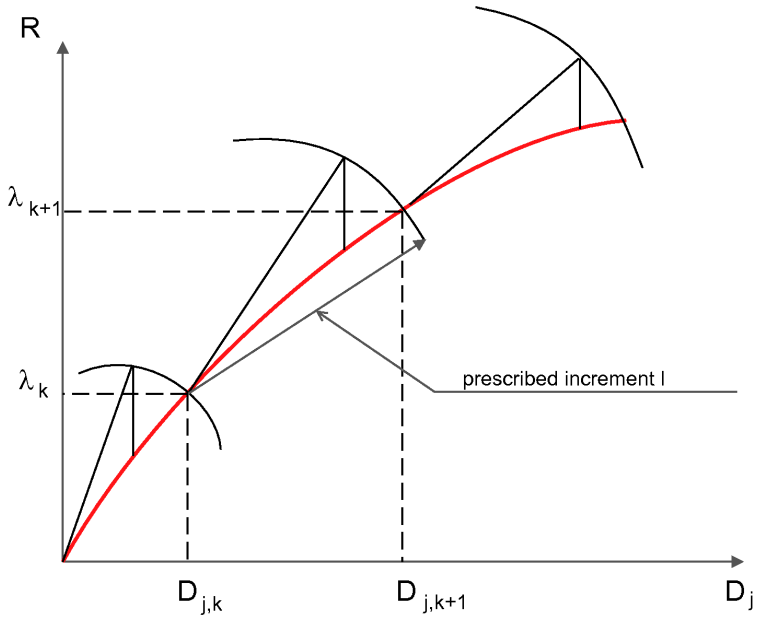

FIGURE 2.6: The Arc-Length Method

The basic idea behind arc length methods is that instead of keeping the load (or the displacement) fixed during an incremental step, both the load and displacement increments are modified during iterations. the 'arc length' of the combined displacement-load increment is controlled during equilibrium iterations. An additional unknown $\Delta\lambda$ is introduced to the n_{dof} incremental displacements $\{\Delta D\}$, and so an additional equation is required to obtain a unique solution to $\{\Delta D\}$ and $\Delta\lambda$. A constraint scalar equation is introduced:

$$\{C(\Delta Z)\} = \left\{C(\Delta\lambda, \Delta D)^T\right\} = 0 \tag{2.5}$$

in which the 'length' of the combined displacement-load increment is prescribed:

$$l^2 = \{\Delta D\}^T \{\Delta D\} + \psi^2 \Delta\lambda^2 \tag{2.6}$$

where ψ is a scaling parameter ($\{\Delta D\}$ and $\Delta\lambda$ have different dimensions).

2.2.4 Material Nonlinearity

2.2.4.1 Introduction

Linear elastic FE analysis is based on linear constitutive stress-strain equations:

$$\{\sigma\} = [D]\{\epsilon\} \tag{2.7}$$

in which the terms of material matrix $[D]$ are expressed as functions of constant values of modulus of elasticity and Poisson's ratio. The constant D matrix leads to a constant stiffness matrix $[K], which is for strain - displacement relationship$

$$\{\epsilon\} = [B]\{d\} \tag{2.8}$$

given by

$$[K] = \int_V [B]^t [D][B] \; dV \tag{2.9}$$

Departure from linear elasticity implies that the linear elastic constitutive equations are no longer valid, as the material matrix is no longer constant. The non-constant material matrix $[D]$ represents nonlinear constitutive equations corresponding to the adopted nonlinear material model. Consequently, the conditions of equilibrium derived in FEM from principle of virtual displacements become nonlinear. They are solved as described in the previous section, by dividing the load into increments and performing equilibrium iterations. For each load increment, stress iterations must be performed, as the material matrix is a function of strain. The strain is unknown a priori and will be computed only. Material nonlinearities are often combined with geometrical and/or boundary nonlinearities.

One type of nonlinear material law is the nonlinear elastic material which is used to describe rubber-like materials and will not be discussed in this section.

2.2.4.2 Elastoplastic material model

Experiments indicate that linear elastic model is acceptable only within a limited range of stress. Until the yield stress (for Steel S235 given by $\sigma_y = 235MPa$) the deformations are elastic and stress-strain relation may be described as 2.7. When the stress level exceeds the yield stress, an elastoplastic constitutive law governs the relationship between increments of stress and strain. Approximate stress-strain curves are usually used in analysis. Bilinear approximation defined by yield stress, modulus of elasticity E and tangential modulus E_T is shown in Figure 2.7. If $E_T = 0$, the material model is elastic-perfectly plastic. If $E_T \neq 0$ the material model assumes strain hardening.

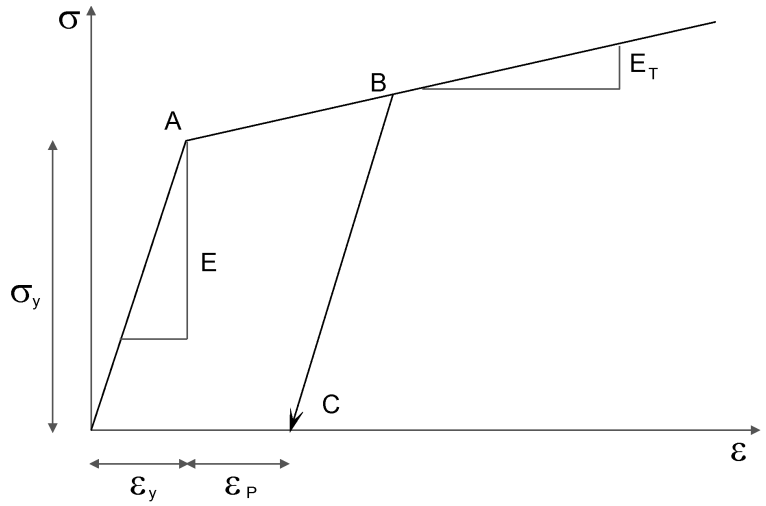

FIGURE 2.7: Elastoplastic model with linear strain hardening

In a mathematical description, onset of yielding may be represented by a scalar function termed the yield function F. The Von Mises yield criterion states that yielding occurs when

$$F = (\sigma_1 - \sigma_2)^2 + (\sigma_2 - \sigma_3)^2 + (\sigma_3 - \sigma_1)^2 - 2\sigma_y = 0 \tag{2.10}$$

where σ_1, σ_2 and σ_3 are principle stresses and σ_y is the yield stress value.

Any yield condition that is function of stress tensor components and material parameters

$$F(\sigma, K) = 0 \tag{2.11}$$

defines a yield surface in principal stress space, see Figure ??. Stress points that lie inside the yield surface are associated with elastic stress states whereas those that lie on the surface represent plastic stress states. No stress point can be outside the yield surface 2.8.

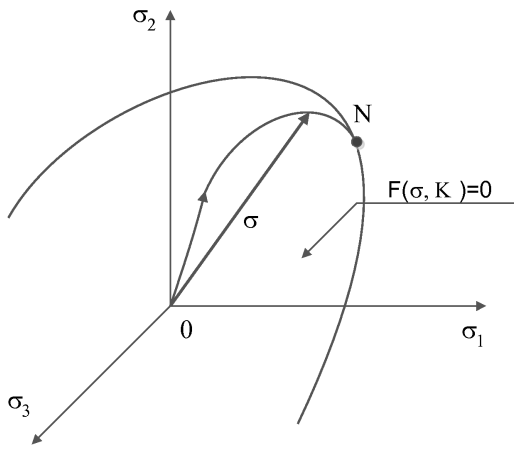

FIGURE 2.8: Yield surface

For a perfectly plastic material, the yield surface remains unchanged during plastic deformation. For a strain hardening material, plastic deformation produces a change in shape and position of the yield surface. This means that initial yield surface is gradually replaced by the subsequent yield surfaces. A modified yield function is adopted which has a form such as

$$F\left(\sigma, \epsilon^P, K\right) = 0 \tag{2.12}$$

This yield function depends on the stresses but also the plastic strains and a hardening parameter K. The way in which the plastic strains modify the yield function is defined by hardening rules:

- An isotropic hardening law implies that the yield surface increases in size but maintains its original shape under loading conditions. Schematic representation of isotropic hardening for uniaxial and biaxial stress state is shown in Figure 2.9.

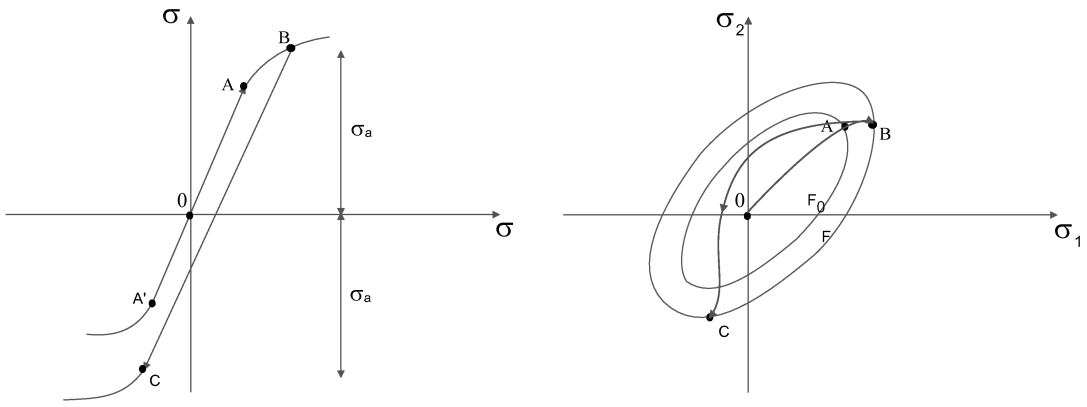

FIGURE 2.9: Isotropic hardening

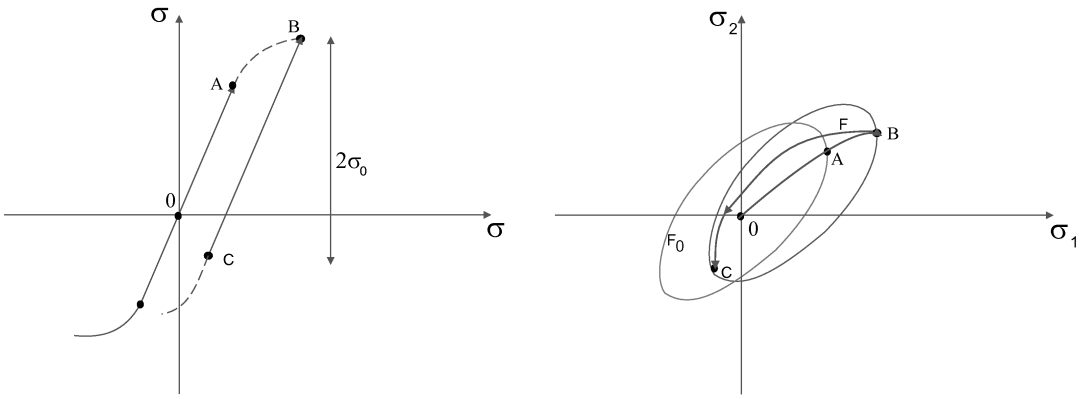

FIGURE 2.10: Kinematic hardening

- In kinematic hardening, the original yield surface is translated to a new position in stress space with no change of its shape and size as shown in Figure 2.10. Kinematic hardening is important for modeling cyclic behaviour.

- The combination of the two principal hardening laws leads to a mixed hardening law, where the initial yield surface both expands and translates as a consequence of plastic flow.

Plasticity in ANSYS

In ANSYS, plastic analysis is much like a transient problem where instead of time stpes we have load steps. If plastic response is anticipated in an analysis, the loads should be applied as a series of small incremental load steps or time steps, so that the model can follow the load-response path as closely as possible. The automatic time stepping feature available in the program will respond to plasticity after the fact, by reducing the load step size after a load step in which a large number of equilibrium iterations is

performed or in which a plastic strain increment greater than 15 Percent is encountered. If too large a step is taken, the program will bisect and re-solve using a smaller step size.

Elements have to be chosen that support plasticity. For every material elastic modulus, poisson's ratio, and yield stress has to specified. Also, a stress-strain curve of the material has to be defined by the user.

Several options are available for describing plasticity behavior:

- The Bilinear Kinematic Hardening (BKIN) option assumes the total stress range is equal to twice the yield stress, so that the Bauschinger effect is included. This option is recommended for general small-strain use for materials that obey von Mises yield criteria (which includes most metals). It is not recommended for large-strain applications.
- The Multilinear Kinematic Hardening (MKIN) option uses the Besseling model, also called the sublayer or overlay model, so that the Bauschinger effect is included. This option is not recommended for large-strain analyses.
- The Multilinear Isotropic Hardening (MISO) option uses the von Mises yield criteria coupled with an isotropic work hardening assumption. This option is not recommended for cyclic or highly nonproportional load histories in small-strain analyses. It is, however, recommended for large strain analyses. The MISO option can contain up to 20 different temperature curves, with up to 100 different stress-strain points allowed per curve. Strain points can differ from curve to curve
- The Bilinear Isotropic Hardening (BISO) option is like the multilinear isotropic hardening option, except that a bilinear curve is used instead of a multilinear curve. This option is often preferred for large strain analyses.
- The Anisotropic (ANISO) option allows for different bilinear stress-strain behavior in the material x, y, and z directions as well as different behavior in tension, compression, and shear. This option is applicable to metals that have undergone some previous deformation (such as rolling). It is not recommended for cyclic or highly nonproportional load histories since work hardening is assumed. The yield stresses and slopes are not totally independent. [17]

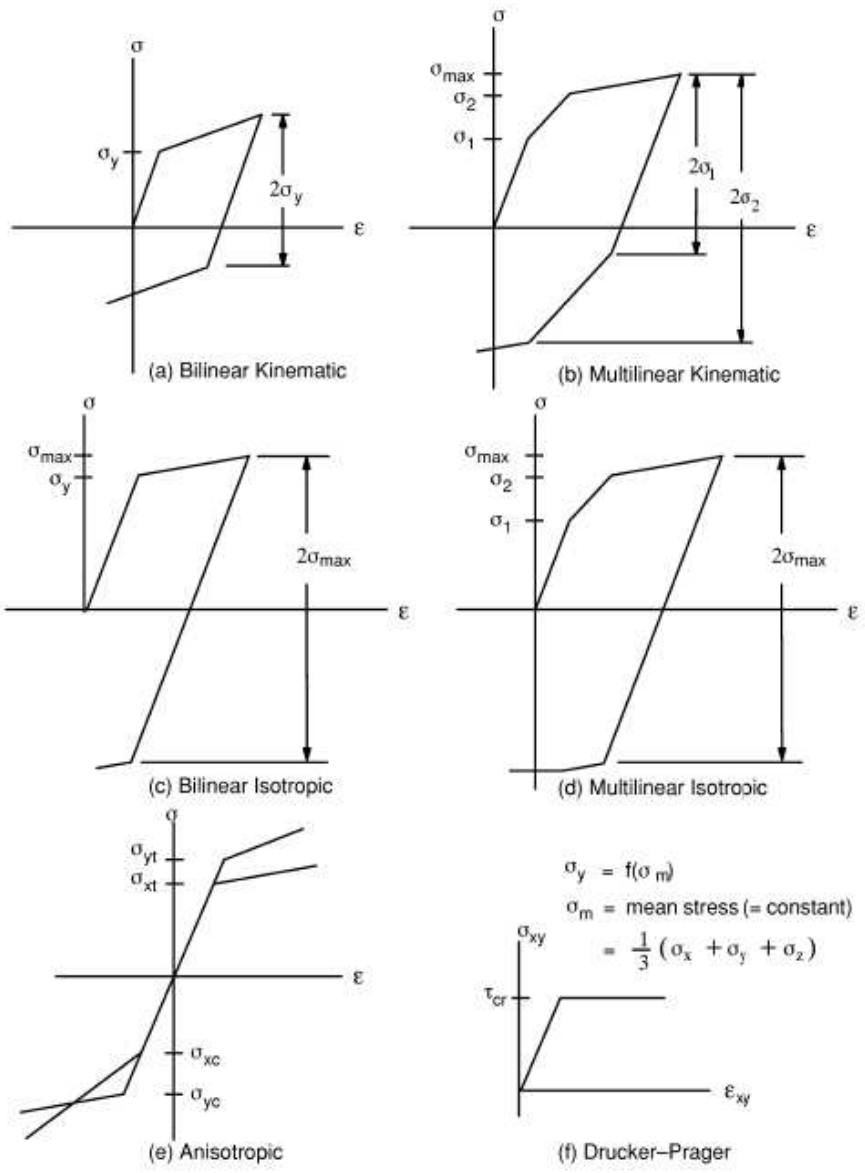

FIGURE 2.11: Kinematic hardening

2.2.5 Geometric Nonlinearity

2.2.5.1 Introduction

Geometric nonlinear effects are caused by gravity loads acting on the deformed configuration of the structure, leading to an increase of internal forces in members and connections. There are 2 effects to be distinguished: $P-\delta$ effects, which cause deformations along the members, measured relative to the member chord, and $P-\Delta$ effects, measured between member ends and commonly associated with story drifts in buildings. Provided that members conform to the slenderness limits for special systems in

high seismic regions, $P-\delta$ effects do not generally need to be modeled in nonlinear seismic analysis. On the other hand, $P-\Delta$ effects must be modeled as they can ultimately lead to loss of lateral resistance, ratcheting (a gradual build up of residual deformations under cyclic loading), and dynamic instability.

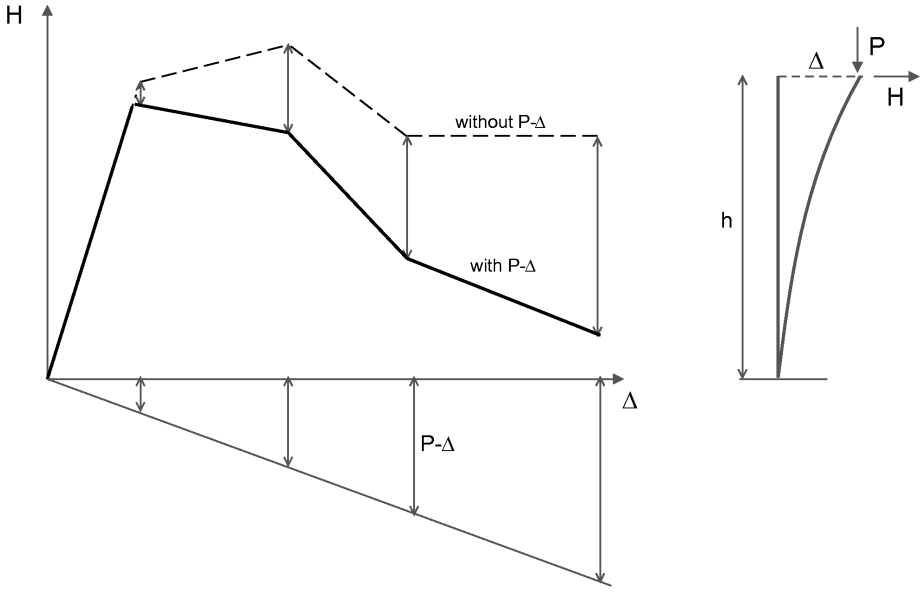

FIGURE 2.12: Force-deformation curve with and without $P-\Delta$ effect [1]

In a static sense the P-delta effect can be visualized as an additional lateral loading that causes an increase in member forces and lateral deflections, reduces the lateral load resistance of the structure, and may cause a negative slope of the lateral load-displacement relationship at large displacements. Shown in Figure 2.12 is an idealized base shear versus drift curve of a cantilever structure with and without $P-\Delta$ effects. If the gravity load is large the stiffness reduction (shown by the negative slope) is significant and contributes to loss of lateral resistance and instability. Therefore the gravity load-deformation $P-\Delta$ effect must be considered directly in the analysis, whether static or dynamic. This means that the gravity loads of the entire building must be present in the analysis, and appropriate $P-\Delta$ analysis techniques should be introduced in the structural model.

2.2.5.2 $P-\Delta$ effect on a SDOF System

The effects of large displament will be described on a single degree of freedom system. For a bilinear SDOF System the $P-\Delta$ effect can be represented as illustrated in Figure

2.13. It consists of a mass m, with a weight force P, supported by a rigid column of height h, with a flexural spring at its base. A lateral force, V, applied to the mass causes a deflection, Δ. It is assumed that the base spring is bilinear. The initial stiffnes of this curve is K_0, which reduces to $\alpha' K_0$ after yield occurs at a lateral force V_y^0. The nonlinear behavior of the oscillator under an earthquake ground motion is governed by its natural period of vibration T, the fraction of critical damping ξ, the strain hardening ration α' and th evalue of the non-dimensionalised yield strength V_y^0/mg of the spring. The ductility demand is given by $\delta_{max}^0/\delta_y^0$, where δ_y^0 is the deflection at yield and δ_{max}^0 is the maximum deflection.

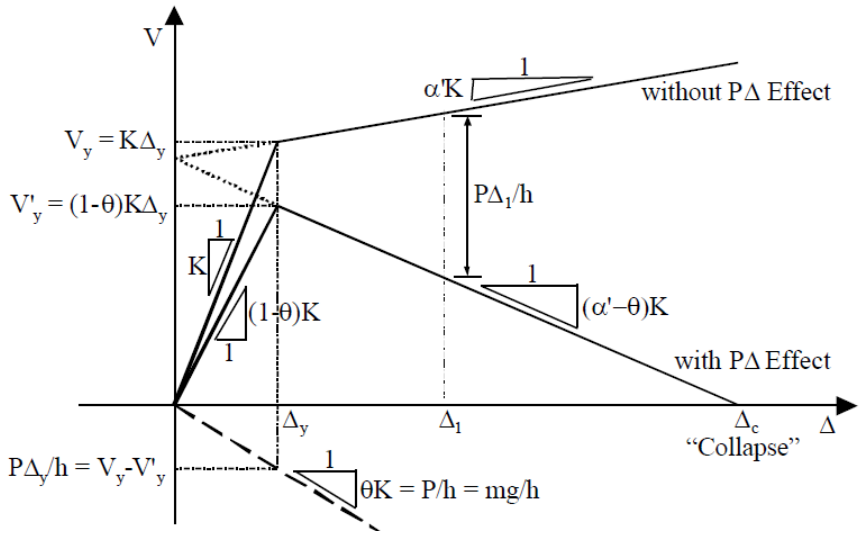

FIGURE 2.13: SDOF Lateral Force-Displacement Relationship with and without $P-\Delta$ effect.
[]

The inclusion of the vertical weight P into the oscillator model reduces the lateral stiffness by P/h and the effective strength for resisiting lateral forces to $V_y^0 = P\delta_y^0/h$. The lateral force versus deflectoin of the system with $P-\Delta$ effects is represented by the dashed line.

The nondimensional ratio of the $P-\Delta$ over-turning moment to the resisting strength, which has been defined as the stability factor θ is given by:

$$\theta = \frac{P\delta}{Vh} \tag{2.13}$$

The reduction in effectice stiffness of the oscillator caused by he influence of the $P-\Delta$ load means that the period of oscillation is increased from T to T'. As the period inversely

proportional to the square root of the effective initial stiffness, the stability coefficient θ may alternatively be calculated as

$$\theta = 1 - \left(\frac{T}{T'}\right)^2 \tag{2.14}$$

The stability coefficien is used to describe the decrease in strength and stiffness. The elastic stiffness K is rdeuced to $(1-\theta)K$ and the post-elastic stiffness $\alpha' K$ is reduced to $(\alpha' - \theta)K$. In this formulation α' is the strain-hardening ratio of the system without $P-\Delta$ effects, and $(\alpha' - \theta)$ is the ratio with $P-\Delta$ effects, which is denoted here as α. If $\theta >'$, then α becomes negative and for such a case the system reaches a state of zero lateral resistance (termed as "collapse") at a displacement of Δ_c. The maximum lateral strength of thesystem with $P-\Delta$, V_y', is the strength of the system without $P-\Delta$reduced by a factor of $(1-\theta)$.

2.2.5.3 Geometric Nonlinearities in ANSYS

There are two types of geometric nonlinearities: large deflections with small strain and large deflection with large strain. By issuing NLGEOM,ON (GUI path Main Menu-Solution-Analysis Options), large strain effects in those element types that support this feature are activated. The large strain feature is available in most of the solid elements (including all of the large strain and hyperelastic elements), as well as in most of the shell and beam elements.

What is of interest in a nonlinear pushover analysis is the large deflection-small strain solution. This feature is available in Ansys for all beam and most shell elements, as well as in a number of the nonlinear elements. Issuing NLGEOM,ON (Main Menu-Solution-Analysis Options) activates large deflection effects for those elements that are designed for small strain analysis. [4]

2.2.6 Nonlinear Connections

2.2.6.1 Introduction

Another source of nonlinearity in structures is the nonlinear boundary condition. In steel structures the most important are the connections which are commonly treated as either perfectly pinned or perfectly rigid. In reality the behavior is semi-rigid which influences strongly the overall response of the structure. It is particularly important to include the effects of connection flexibility in the analysis of building systems for use in limit state design methods and in evaluating the seismic risk of structures. [3]

2.2.6.2 Modeling the Nonlinear Connection

In most investigations only in-plane behavior of connections is considered. Usually the connection behavior is modeled by a nonlinear equation for moment-rotation response which is calibrated to test data and normalized for use in design. One model which is often used in analysis is the model of Richard and Abbott, which uses a nonlinear equation to describe the moment-rotation behavior of the connection:

$$M = \frac{(K_e - K_p)\theta}{\left(1 + \left|\frac{(K_e - K_p)\theta}{M_0}\right|^n\right)^{1/n}} + K_p\theta \tag{2.15}$$

where M is the moment corresponding to the connection rotation, θ. The parameters, K_e, K_p and M_0, are independent variables which are related to the moment-rotation behavior as shown in Figure 2.14, and n controls the shape of the curve. This model encompasses more simple models: equation 2.15 becomes a simple linear model if $K_e = K_p$, an elastic-plastic model if $K_p = 0$, and a bilinear model if n is large.

The four parameters may be determined using analytic formulations for the connection strength and stiffness if the connection details are known. Or they may be determined through curve fitting and optimization if test data are known. The parameters can be found in literature for the various connection types.

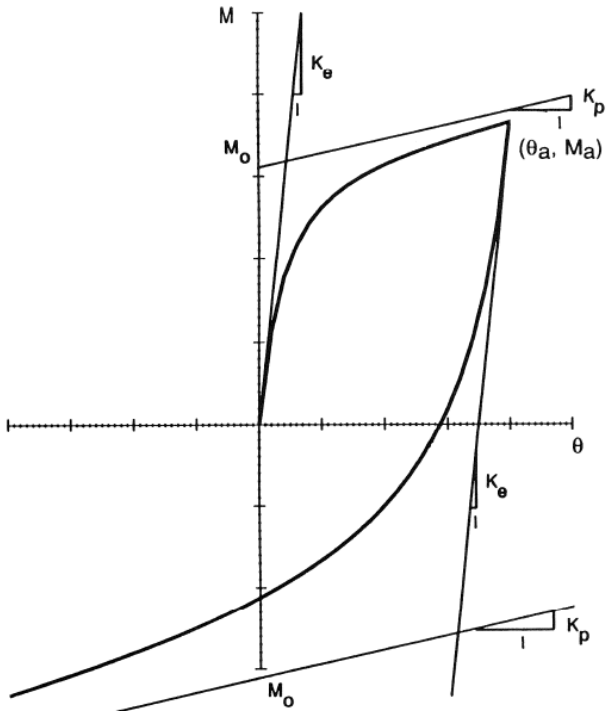

FIGURE 2.14: Moment-rotation Model for Inelastic Connection Response [3]

2.2.6.3 Connections in ANSYS

Ansys connects the different multibody components through joint elements. The MPC 184 family of elements serves to connect the flexible or rigid components to each other. An MPC 184 joint element is defined by two nodes with six degrees of freedom at each node (for a total of 12 DOFs). The relative motion between the two nodes is characterized by six relative degrees of freedom. Different kinds of joint elements can be configured by imposing appropriate kinematic constraints on these six relative degrees of freedom. For example, to simulate a revolute joint, the three relative displacement degrees of freedom and two relative rotational degrees of freedom are constrained, leaving only one relative degree of freedom available (rotation around the revolute axis).

Stops or Limit constraints in joints can be imposed on the available components of relative motion between the two nodes of a joint element. The stops or limits essentially constrain the values of the free DOFs within a certain range. The SECSTOP command is used to specify the values.

The stiffness and damping behavior of joint elements can be specified. They are associated with the free or unrestrained components of relative motion of the joint elements. In the case of linear behavior, the values are specified as coefficients of a 6×6 elasticity

matrix using the TB,JOIN command with $TBOPT = STIF$ or $TBOPT = DAMP$. The nonlinear stiffness and damping behavior is specified using the TB,JOIN command with an appropriate TBOPT label. In the case of nonlinear stiffness, relative displacement (rotation) versus force (moment) values are specified using the TBPT command. An example of a nonlinear curve is given in Figure 2.15. Nonlinear stiffness or damping behavior can be specified independently for each of the unrestricted components of relative motion. citekohnke2001ansys

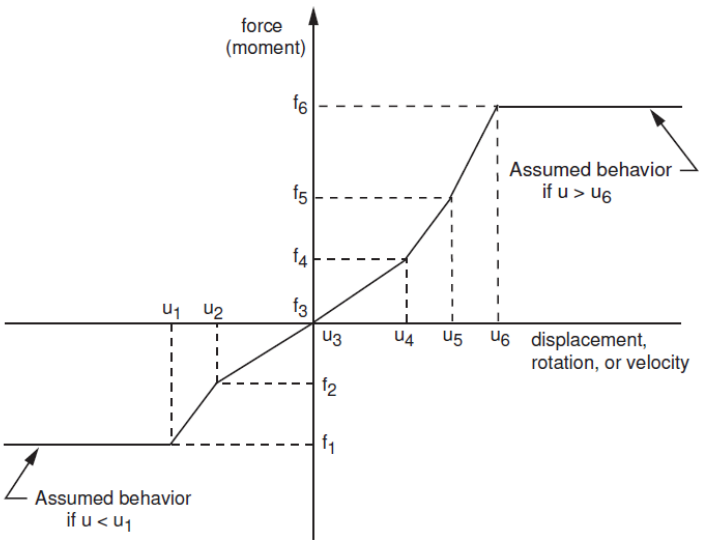

FIGURE 2.15: Nonlinear stiffness and damping behavior for joints [4]

2.3 Element Types in ANSYS

2.3.1 Introduction

ANSYS supports a large library of beam and shell elements with wide applicability: composites, buckling and collapse analysis, dynamics analysis and nonlinear applications.

The recent 180-series elements were designed and developed for large deformation analysis with a large number of advanced elements technology and and a rich nonlinear support. During the development, consistency and generality were the main theme, hence fewer assumptions were made. They are natural candidates for nonlinear analysis such as finite strain and large rotation analysis or hystory dependent and independent materials.

The beam elements (BEAM 188 and BEAM 189) enable the reduction in dimensionality of the problem. After definition of cross section by the user, a finite element cross-section analyzer calculates inertias, shear centers, shear flow, warping rigidity, torsion constant. Arbitrary profiles can be sketched. Depending on the solution that is sought, the mesh quality for the section can be as well specified. There are two types of cross sections: thin wall sections (CTUBE, CHAN, I, Z, L, T, HATS and HREC) and solid sections (RECT, QUAD and CSOLID). The thin wall sections have a minimum of two integration points through thickness, so results produced using thin wall sections should be acceptable for materially nonlinear analysis. However, when doing a plasticity analysis, the cell defaults may need to be changed for the solid sections (for example: refinement at the edges). All elastoplastic, hypo-viscoelastic material models may be used. Different types of materials within the same cross section may be used as well. [4]

A comparison shows that the reduction in CPU time while using beam elements instead of solid elements is substantial, while the approximation of results is minimal, see Figure 2.16.

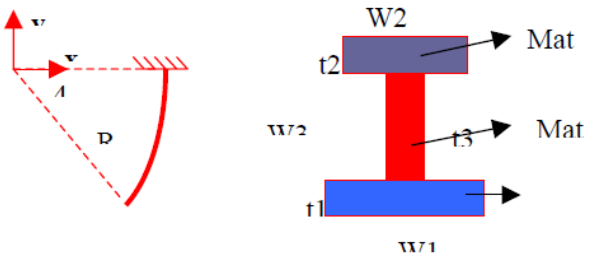

	BEAM189 (NDOF=96)		BEAM189 (NDOF=192)		SOLID186 (NDOF=18900)
Max. displacement	Value	% diff.	Value	% diff.	Reference value
Ux	19.664	0.2	19.666	0.2	19.625
Uy	24.819	1.9	24.822	1.9	25.310
Uz	54.486	0.5	54.490	0.5	54.769
CPU Time	82.610		115.460		4587.850

FIGURE 2.16: Nonlinear analysis of a curved beam: comparison with solid elements [4]

2.3.2 Beam 188

BEAM 188 is a linear finite strain beam. They are one-dimensional 2-node line elements in space. The geometry, node locations, and the coordinate system for this element are shown in Figure 2.17. BEAM188 is defined by nodes I and J in the global coordinate system. Node K is always required to define the orientation of the element. [4]

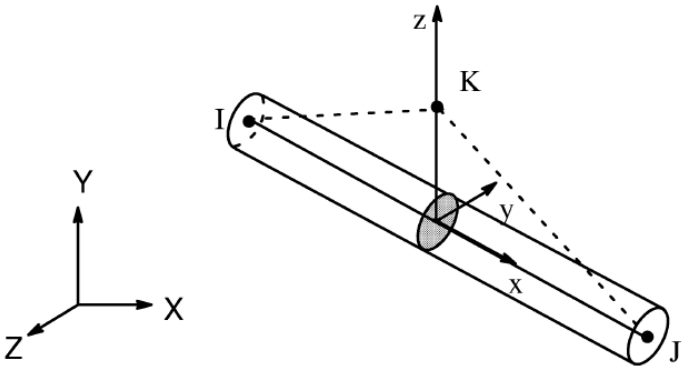

FIGURE 2.17: Beam 188- Finite Strain Linear Beam [4]

Properties:

- The BEAM188 element is suitable for analyzing slender to moderately stubby/thick beam structures. The element is based on Timoshenko beam theory which includes shear-deformation effects. The element provides options for unrestrained warping and restrained warping of cross-sections.
- it is based on Timoshenko beam theory, which is a first-order shear-deformation theory: transverse-shear strain is constant through the cross-section (that is, cross-sections remain plane and undistorted after deformation).
- it includes stress stiffness terms, by default, in any analysis with NLGEOM,ON. The stress stiffness terms provided enable the elements to analyze flexural, lateral and torsional stability problems (using eigenvalue buckling or collapse studies with arc length methods).
- it can be used with any cross section defined. Elasticity and isotropic hardening plasticity models are supported (irrespective of cross section subtype).

2.3.3 Beam 189

The element is a quadratic three-node beam element in 3-D, see Figure 2.18. BEAM189 is defined by nodes I, J, and K in the global coordinate system. With default settings, six degrees of freedom occur at each node; these include translations in the x, y, and z directions and rotations about the x, y, and z directions. An optional seventh degree of freedom (warping magnitude) is available. The element is well-suited for linear, large rotation, and/or large-strain nonlinear applications.

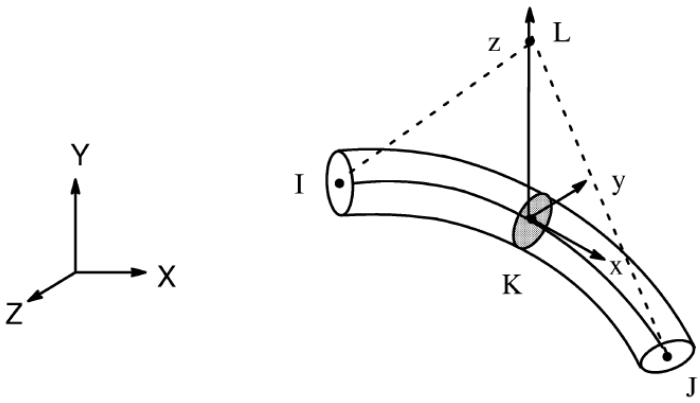

FIGURE 2.18: Beam 189- Finite Strain Quadratic Beam [4]

The element is a one-dimensional line element in space. The cross-section details are provided separately. Each section is assumed to be an assembly of a predetermined number of nine-node cells, see Figure 2.19. Each cross-section cell has four integration points and each can be associated with an independent material type. The number of cells in the cross-sections influences the accuracy of section properties and ability to model nonlinear stress-strain relationship through the cross-section. The element has a nested structure of integration (along the length and in the cross-section).

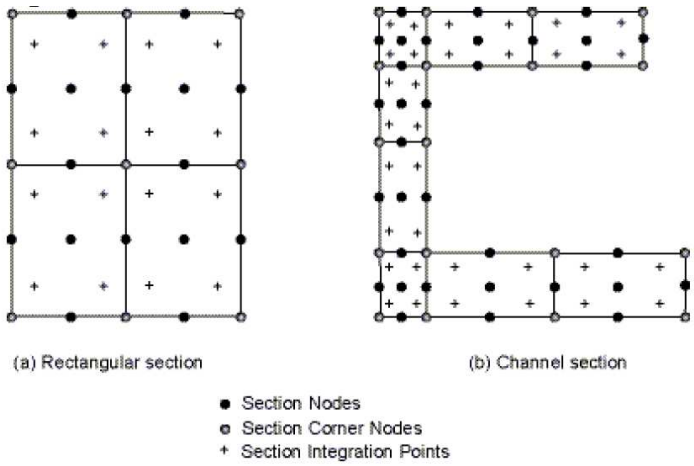

FIGURE 2.19: BEAM188 and 189 Cross Section Models [4]

When the material associated with the elements has inelastic behavior or when the temperature varies across the section, constitutive calculations are performed at the section integration points. For more common elastic applications, the element uses precalculated properties of the section at the element integration points. However, the stresses and strains are calculated in the output pass at the section nodes.

Forces are applied at the nodes, which also define the element x-axis. The nodes should therefore be located at the points where the forces will be applied. Pressures may be input as surface loads on the element faces. Positive normal pressures act into the element. Lateral pressures are input as force per unit length. End pressures are input as forces.

2.3.4 Conclusion

While analyzing a multistory steel structure it is preferable to find ways of reducing the solution time and effort. Using shell or solid elements may render a more accurate solution in terms of presenting regions of member plastification and degrading of elements but are not necesarry for computing the overall response of the structure. The Beam Elements 188 and 189 offer a wide range of possiblities for capturing the nonlinear reponse of a building while reducing the CPU time noticeably. They represent a significant move towards true reduction of dimensionality of the problem.

Chapter 3

Case Studies

In the previous two chapters the theory behind pushover analysis and the implementation in a nonlinear finite element program have been discussed. In this chapter steel frame structures will be analyzed in order to asses the implementation of the nonlinear problem in ANSYS. First a simple one bay steel frame will be subjected to vertical and lateral loads and the response of the structure in Ansys will be compared with the exact analytical solution. Further different types of modelling of the structure will be discussed. Subsequently a 9 story building will be analyzed and a pushover analysis will be performed. The results will be compared to the ones available in previous studies.

3.1 Single Story, One Bay Steel Frame

First a simple example of a steel frame is analyzed in order to assess the modeling quality and results in ANSYS and to proceed to a more complex structure with confidence. Moreover, a decision will be taken if modeling of the structure with beam elements renders meaningful results and is a suitable tool for the subsequent pushover analysis of steel frame structures.

3.1.1 Description of the Geometry

The Geometry to be analyzed is a single bay steel frame. All member connections are fixed, as well as the boundary conditions. The structure is 4m in width and 2m in height.

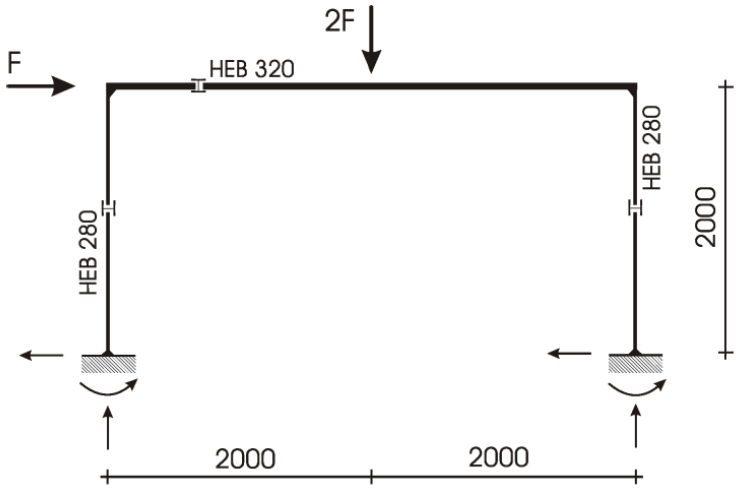

FIGURE 3.1: Steel Frame Dimensions [mm].

Figure 3.1 illustrates the dimensions and loads. What is inquired is the ultimate force F that can be supported by the structure, in other words the collapse load. Further, the location of plastic hinges should be detected.

3.1.2 Modeling in ANSYS Workbench

The structure will be modeled in ANSYS Workbench with BEAM 189 Elements. As presented earlier, this elements can capture nonlinearities, material as well as geometric and should provide a viable simplification of the problem. Modeling in ANSYS Workbench implies a series of steps:

A. First a static structural analysis has to be selected

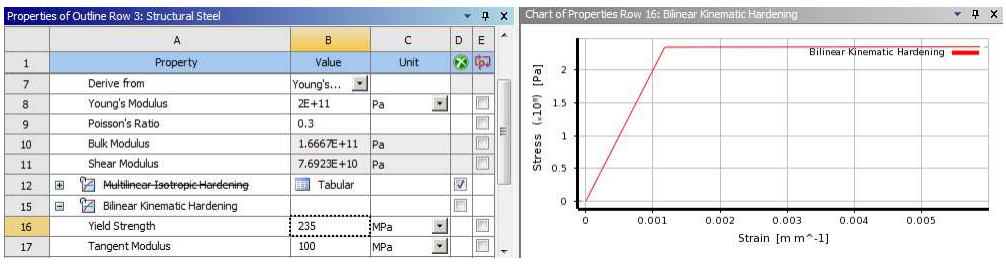

FIGURE 3.2: Material properties.

B. In the field with engineering data a material model is specified. In this example a material which captures the material nonlinearity of steel has to be defined. The material has a Young's modulus of 2e11 Pa, a Poisson's ratio of 0.3. Further a bilinear kinematic hardening model is selected with a yield strength of 235 MPa and a tangent modulus of 100 MPa. A tangent modulus different from zero provides a more stable solution and allows the tracking of the deformation of the structure into the nonlinear range. It allows the determination of the collapse load, not only the yield load of the structure. The properties of the material can be visualized in Figure 3.2.

C. In the next step the geometry of the structure is created in ANSYS Design Modeler. Points are defined which are further connected through lines. Cross section properties are manually defined. For every line the specific cross section is selected which enables the creation of line bodies. In design modeler it is determined the line bodies are connected to each other by building a part or by defining joints in ANSYS Mechanical and joint properties between each member. For fixed connections both are suitable and render the same results.

D. The geometry is then loaded in ANSYS Mechanical. Connections are specified through joint members. Two types of connections are suitable for the analysis of steel frame structure. Either the fixed joints for rigidly fixed connections or revolute joints in order to simulate pin joints between two members. For the revolute joints a torsional stiffness and a torsional damping can be specified in order to model a semi-rigid connection between two members. For the presented problem simple fixed joints are selected. This creates an MPC 184 element which is used to model a rigid constraint between two deformable bodies or as a rigid component used to transmit forces and moments. This element is well suited for linear, large rotation, and/or large strain nonlinear applications.

The Mesh properties are specified for the line bodies. It can be done automatically or by apllying mesh control. For this example the mesh generation is left on automatic with relevance center on medium which generates a fine mesh in order to capture the spread of plasticity throughout the member length.

In the static structural branch the supports and forces are specified: fixed supports for the end of the beams, a displacement support for the whole structure with Uz=0, which

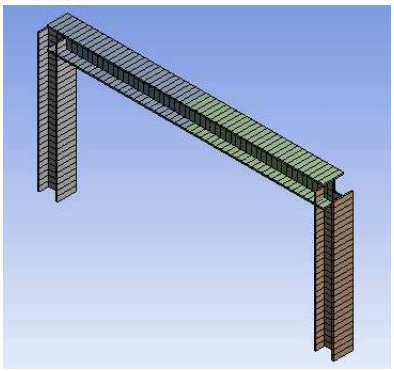

(A) Meshed Frame.

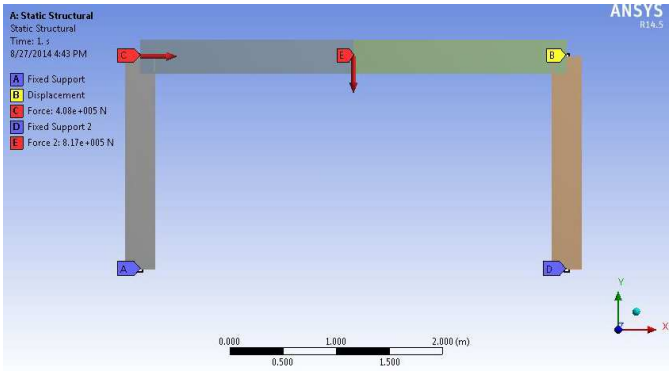

(B) Forces and Supports.

should prevent the structure from buckling and a horizontal and vertical force which act on the frame.

In the solution branch the data of interest is selected: total deformation, force and moment reaction for the supports, axial force, shear force and bending moment for the frame. Further a chart is generated in order to plot the base shear vs. roof displacement curve which will be of interest in further analysis.

For a nonlinear problem the selection of the analysis settings under the static structural branch are fundamental. This includes the step controls as well as the solver and nonlinear controls. In step controls the automatic time stepping is turned on. This allows ANSYS to determine appropriate sizes to break the load steps into. Decreasing the step size usually ensures better accuracy, however, this takes time. The Automatic Time Step feature will determine an appropriate balance. It also activates the ANSYS bisection feature which will allow recovery if convergence fails. The number of substeps is specified: initial substeps are set on 40, minimum substeps on 20 and maximum substeps on 50. This will set the initial substep to 1/40 th of the total load and it stops the program if the problem doesn't converge after 50 substeps. This will apply the load gradually and will allow tracking of the deflected shape and the beginning of steel yielding. In the solver controls the large deflection can be turned on and off, depending whether geometric nonlinearities are taken into account or not. Further in the nonlinear controls the stabilization method is set on constant, with automatic values set by the program, which will enable a more stable solution and will enhance the convergence. Due to the fact that steel frames are often slender structures, they yield instability problems when the load reaches its buckling value or when nonlinear material becomes unstable.

Instability problems usually lead to convergence difficulties and therefore require the application of special nonlinear techniques. One of this techniques is the nonlinear stabilization which deals with local instabilities as well as global. It can be used together with line search and automatic time stepping. The arc-length method is another way of dealing with the problem, but it poses several restrictions: it doesn't work well with joints as well as with other nonlinear techniques and it prevents only global instability, not local buckling. [4] Its advantage is that it can simulate the negative slope portion of a load-vs.-displacement curve. However this is not required in the present analysis, thus the stabilization method is chosen.

E. Finally, the problem is solved and the results are evaluated.

3.1.3 Results

In this section the results are displayed for the analytical solution and susequently for the solution in Ansys. Results in Ansys are evaluated for a model including material nonlinearity as well as for one including both material and geometric nonlinearity. Finally these results are compared and a conclusion is drawn.

3.1.3.1 Analytical Results

The analytical solution does not take into account geometric nonlinearity.

	HEB 280	HEB 300
N_{pl}	3078,5 kN	3783,5 kN
$V_{pl,z}$	552,5 kN	697,5 kN
$M_{pl,y}$	$360,5kNm = M_{pl}$	$503kNm = 1,4 \cdot M_{pl}$

TABLE 3.1: Plastic internal force limits.

The location of plastic hinge was determined by the minimum of applied force that leads to a collapse mechanism, see Figure 3.3. The internal work is:

$$W_i = M_{pl} \cdot \varphi + 1,4 \cdot M_{pl} \cdot 2\varphi + M_{pl} \cdot 2\varphi + M_{pl} \cdot \varphi \tag{3.1}$$

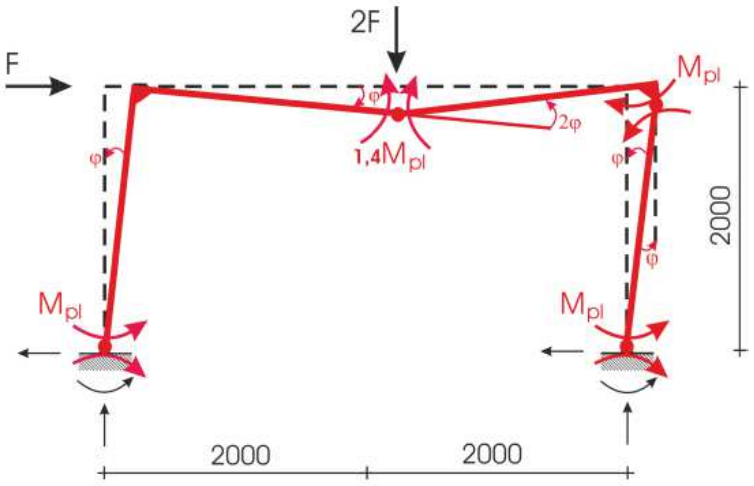

FIGURE 3.3: Plastic hinge formation at collapse load.

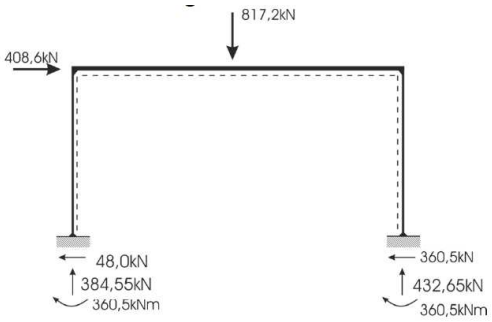

(A) Applied forces and reactions.

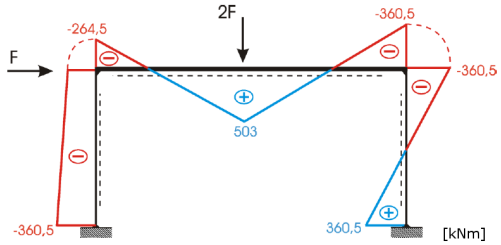

(B) Bending moment diagram.

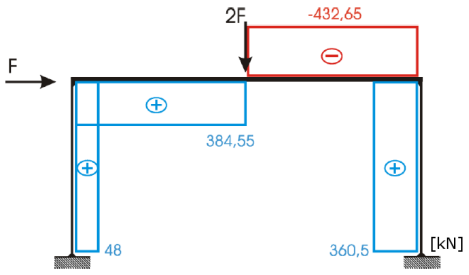

(C) Shear force diagram.

(D) Axial force diagram.

FIGURE 3.4: Reactions, internal forces and moments at collapse load.

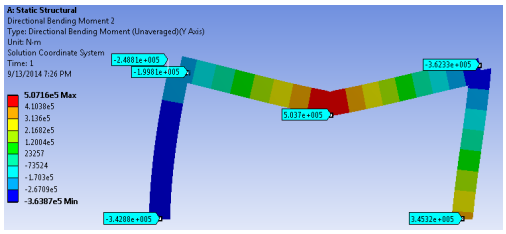

(A) Bending moment.

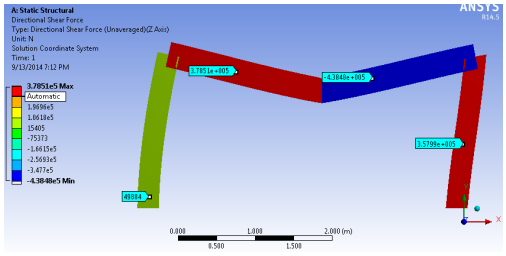

(B) Shear force.

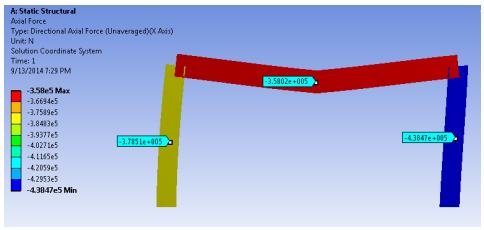

(C) Axial force.

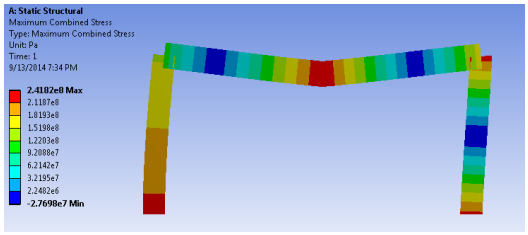

(D) Maximum combined stress.

FIGURE 3.5: Internal forces, moment and stress at collapse load.

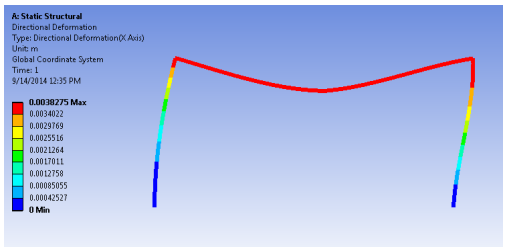

(A) Deformation before collapse load.

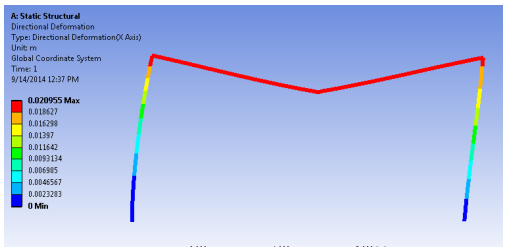

(B) Deformation at collapse load.

FIGURE 3.6: Deformation.

The external work is:

$$W_a = F \cdot 2m \cdot \varphi + 2F \cdot 2m \cdot \varphi \tag{3.2}$$

Setting $W_i = W_a$ leads to the collapse load:

$$F_{pl} = \frac{6,8}{6} \cdot Mpl = 408.6kN \tag{3.3}$$

At the collapse load, the internal forces and moments are then plotted, see Figure 3.4. These results will be compared to the results provided by ANSYS.

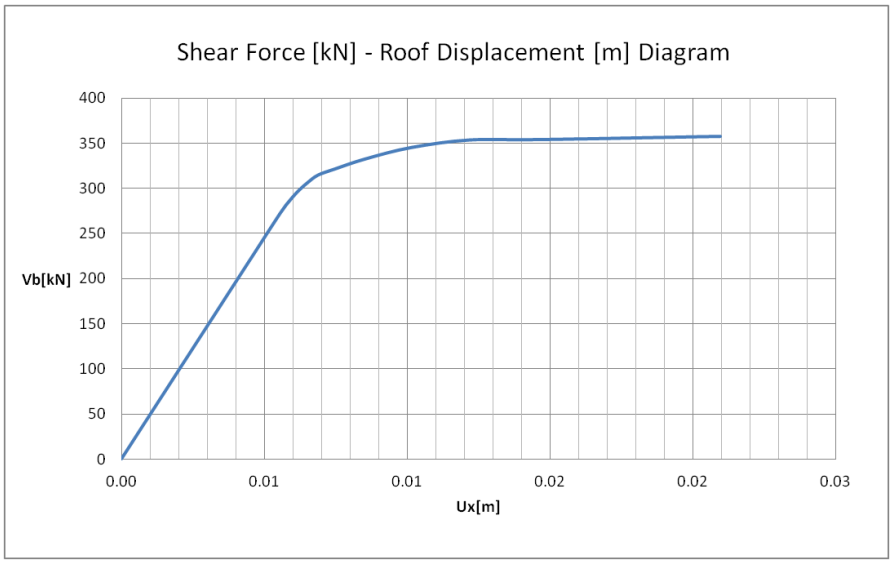

FIGURE 3.7: Shear force vs. displacement chart.

3.1.3.2 Results in ANSYS for Material Nonlinearity

Finding the collapse load in ANSYS is an iterative process. If the load is overestimated, the problem fails to converge and an error message appears, stating that the probe is displaying an unconverged solution. That indicates that the slope of the force- deformation curve is negative and the building collapses.

The bending moment, shear force and axial force diagram are plotted at the collapse load, see Figure 3.5. They are in good accordance with the analytical solution. A slight difference can be observed at the column base, where the plastification occurs before reaching the full plastic moment of the cross section. This may be due to the interaction of moment, shear and axial forces, which was not taken into account in the analytical solution.

Of further interest are the locations of plastic hinges in the model. They can be determined by plotting the maximum combined stress, see Figure 3.5d. The maximum value is 241.8 MPa, which is slightly larger than the yield strength of 235 MPa, due to steel hardening after the onset of yielding. The points where the maximum combined stress exceeds this value indicate the formation of a plastic hinge. This can be visually checked by further plotting the deformed structure before and at collapse load, see Figure 3.6. The deflected shape changes as the load increases and a sharp bend can be observed at the location of plastic hinges.

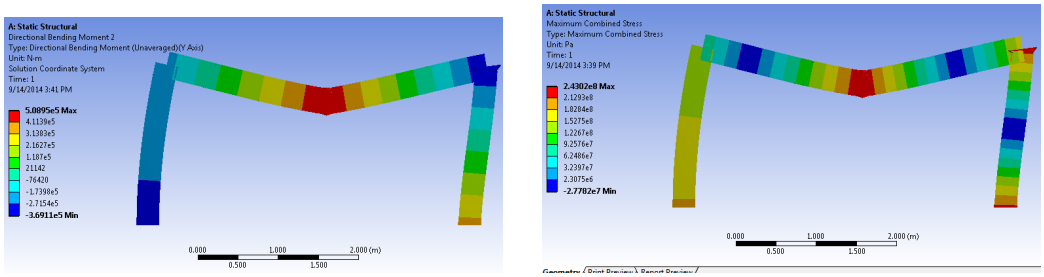

(A) Bending moment. (B) Maximum combined stress.

FIGURE 3.8: Results for the problem including geometric nonlinearity.

Finally a shear force vs. roof displacement chart is plotted, see Figure 3.7, which is essential for a pushover analysis. The middle point of the girder is selected as the control node.

3.1.3.3 Results in ANSYS for Material and Geometric Nonlinearity

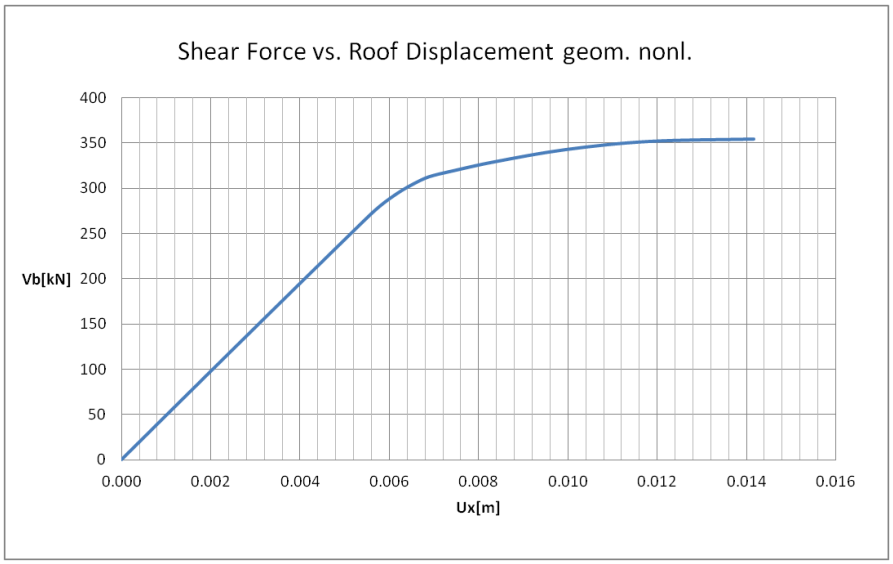

FIGURE 3.9: Shear force vs. displacement chart.

The same procedure is followed for a model including both material and geometric nonlinearity. In order to include geometric nonlinearity, large deflection in solver controls under analysis settings is turned on. The shear force vs. roof displacement chart displayed in figure 3.9 shows that the onset of yielding and the associated displacement and yield strength occurs at approximately same point as in the model which does not include geometric nonlinearity, however the shape of the curve after yielding evolves differently. The slope becomes faster negative and the solution fails to converge sooner,

at 96,5 percent of the collapse load for the model without geometric nonlinearity. This solution is more accurate, however the negative slope portion of the curve is of no interest to the further study. In a modal pushover analysis procedure this portion would be approximated as being perfectly plastic. Moreover a model including geometric nonlinearities poses convergence difficulties due to the associated instability. Figure 3.8 illustrates the bending moment and maximum combined stress at collapse load.

3.1.4 Conclusion

This study has led to the following conclusions:

- Results are quick and in good accordance with the analytical results.
- In the case of fixed connections, both models ,with and without joints, can be used, as they render the same results.
- The automatic time stepping feature together with the other nonlinear features that have been implemented captures very well the force-deformation relationship.
- In order to get better results and enhance convergence a greater number of elements should be used. Moreover, it captures the spread of plasticity along the member length.
- Bilinear material model with tangent modulus different than zero can be used with confidence.
- Location of plastic hinge can be detected by using the plot of maximum or minimum combined stress. Further confirmation results from the deflected shape of the structure.
- Modeling with BEAM elements doesn't provide an insight into the distribution of plastic strain over the cross section and it doesn't allow a visual representation of the formation of plastic hinge as a model consisting of solid elements might do, see figure 3.10. But it does provide the point of onset of yielding and the distribution over the length and the overall impact on the structure, visible in the deflected shape. This is actually the relevant data for a pushover analysis. Furthermore, the computing time by implementing beams is much less then by using solids. Thus, the BEAM 189 element, connected by joints is suitable for further analysis.

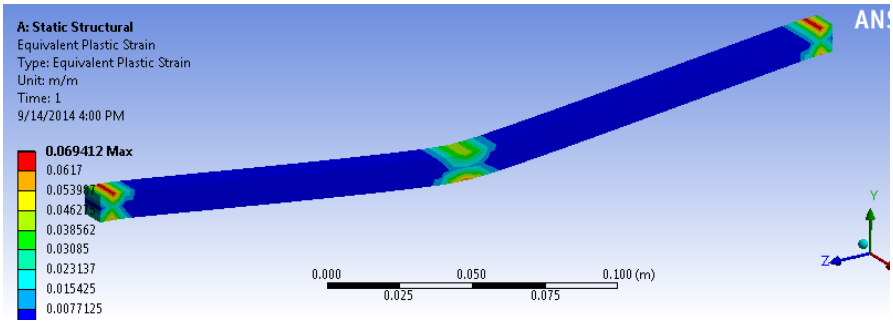

FIGURE 3.10: Shear force vs. displacement chart.

- A model including material as well as geometric nonlinearities renders more exact results. However, due to the idealization of the pushover curve as bilinear and other assumptions inherent to a pushover analysis, an exact solution is not regarded as necessary. In the application of modal pushover analysis procedure, which will be applied for the more complex structure, the negative slope portion of the pushover curve is idealized as being perfectly plastic. Moreover, a model including geometric nonlinearities may pose convergence difficulties. Hence, gravity load and P-delta effects will be excluded from further analysis.

3.2 9 Story Building

3.2.1 Introduction

The presented study focuses on the implementation of a modal pushover analysis in ANSYS. For this endeavor a 9 story steel building was chosen, which is very well documented in literature and for which extensive studies have been carried out. The final goal is to assess the implementation by providing additional results and comparing those to the ones available in previous studies. The main research that has been taken as reference is the one proposed by Goel and Chopra (2004) [7]. The prototype building analyzed in the current endeavor consists of a steel moment-resisting frame designed as a part of the FEMA-funded SAC joint venture project [5]. The Aim of The SAC Joint Venture, formed in 1994, was to develop standards for the repair or upgrading of damaged steel moment frame buildings and for the design of new steel buildings.

SAC commissioned three leading consulting firms to design 3-, 9- and 20-story model buildings according to the local code requirements of three cities: Los Angeles (UBC 1994), Seattle (UBC, 1994), and Boston (BOCA, 1993). The buildings are designed for gravity, wind, and seismic loads with a live load of 2.4 kPa as part of the SAC Steel Project. Even though they are not actually constructed, they meet the local code requirements for Los Angeles, USA region and represent typical low-, medium-, and high-rise steel buildings. A series of analysis have been performed using these models and a large number of results are available in the literature. Many mid- and high rise buildings have steel moment resisting frames (SMRFs) as the primary lateral load resisting system. This type of construction is considered a safe on for earthquake resistance, as steel elements are expected to be able to sustain large plastic deformation in bending and shear. The structure which will be analyzed in this case study is a 9-story structure designed by Brandow & Johnston Associates* for the SAC** Phase II Steel Project. This structure meets seismic code requirements of the 1994 UBC and represents typical medium-rise buildings designed for the Los Angeles, California, region. [5]

3.2.2 Description of the Building

The structural system for the buildings consists of steel perimeter moment resisting frames. A moment resisting frame resists forces in members and joints primarily by flexure and relies on a frame to carry both vertical and lateral loads. Lateral loads are carried primarily by flexure in the members and joints. Theoretically, joints are completely rigid.

To avoid bi-axial bending in corner columns, the exterior bay of the MRF has only one moment-resisting connection. The interior bays of the structure contain frames with simple (shear) connections. The planes of the building are symmetrical.

The 9-story building has plan dimensions of 45.75m x 45.75m (150ft x 150ft) and is 37.19m (122ft) in elevation. It consists of five-bay frames in both N-S and E-W directions spaced at 9.15m (30ft). The building has a basement level, denoted B-1. The height of every level is 3.96 m (13ft) except for the basement level, which is 3.65 m (12ft) and for the first floor, which is 5.49 m (18ft).

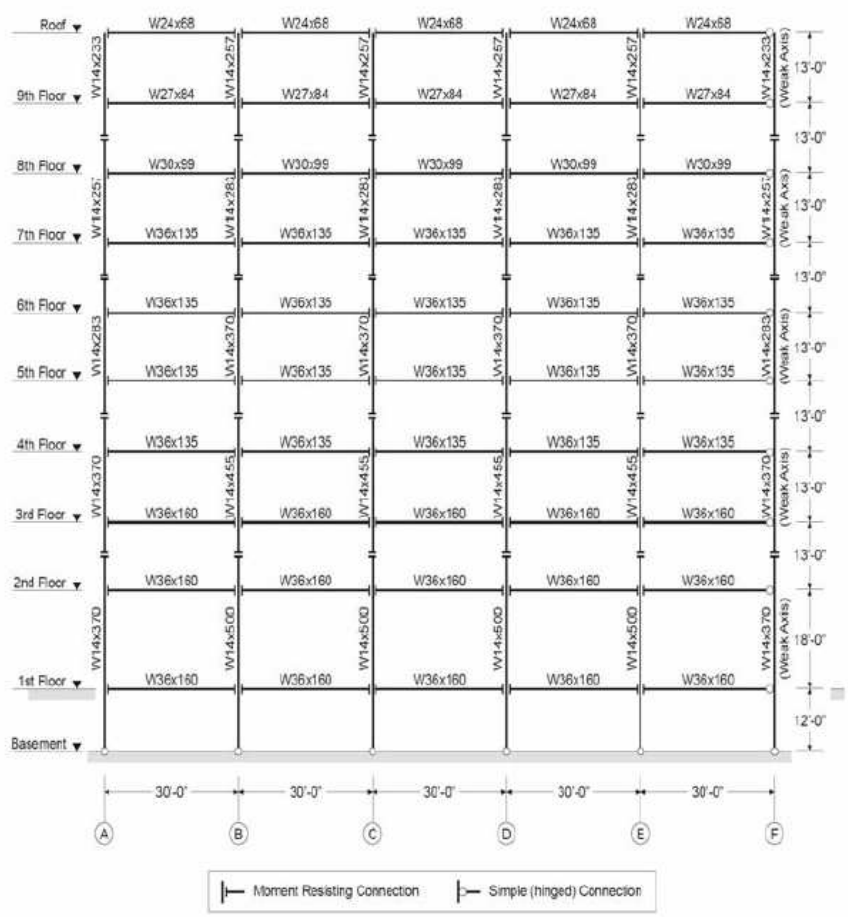

FIGURE 3.11: Building elevation.[5]

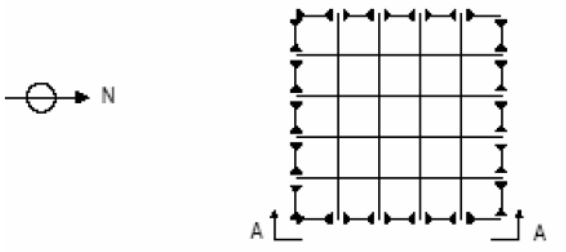

FIGURE 3.12: Building plan. [5]

Monolithic column pieces are connected every two levels through moment- and uplift resistant connections at 1.83m (6ft) above the center-line of the beam to column joint. Concrete foundation walls and surrounding soil are assumed to restrain the structure at the ground level from horizontal displacement. This lateral restraint has been modeled using joint elements developing only compressive forces.

The columns are assumed to be pinned to the ground at B1 and B2 levels respectively. The yield strengths of all columns in the buildings are specified as Fy = 345Mpa. The beams and columns are wide flange and the member dimensions are given in Figure 3.11. The floor system of the buildings is a composite construction with beams having yield strength of Fy = 248 Mpa. The seismic mass of the ground floor is 9.65x105 kg, for first floor is 1.01x106kg, for the second through eighth floor is 9.89x105 kg and the ninth floor is 1.07x106kg. The seismic mass of the entire structure is 9.00x106kg. [5]

3.2.3 Modeling of the Structure

The structure is modeled as a 2 dimensional frame that respresents half of the structure in north-south direction. The frame is given half of the seismic mass of the structure at each floor level. The analytical model employed is a basic centerline model of the moment resisting frame, In this model the beam and columns extend from centerline to centerline. Panel zone effects are neglected. Moments are computed at the connection centerline, which results in a high estimate of moments. In stiffness or lateral displacement calculations the argument for employing such a model is that the use of centerline dimensions compensates for the disregard of panel zone shear deformations. In strength calculation the argument is that an accurate evaluation of strength is desirable but not critical in the evaluation of seismic performance. The other factor of not modeling the panel zone is the complexity and the associated increase in computational effort. [5]

The orientation of the floor beams is also north-south, resulting in uniformly distributed gravity loads on the beams of the MRF and concentrated loads on the columns from the orthogonal beams.

The basement of the structure is modeled as a typical story, however, the basement floor and the ground floor are restrained against lateral displacement. This is employed in

Ansys using a simple support for the columns ends at the basement floor level and a displacement support, with X displacement set to 0, at ground level.

All the frame systems have been modeled including a gravity column to reproduce the overturning effect of weights acting on the other vertical loads resisting members of the structure (P- effects). The latter has been defined by means of an external column composed by pin-jointed elements, with arbitrary sectional properties, pinned at each storey.

A bilinear model has been adopted for steel, defining the post-elastic stiffness ratio (post elastic stiffness/initial stiffness). The post-elastic stiffness ratio was set to 0.008.

Floor Diaphragms transfer the inertial forces to the vertical elements of the framing system. Floor diaphragms are classified as either flexible, stiff, or rigid. The assumption for the present model is that the diaphragm is rigid.

Gravity-load (and P-delta) effects are excluded from all analyses presented in this paper as well as in the paper presented for comparison [7].

The modeling of the structure in ANSYS is similar to the modeling of the one bay steel frame. A difference is in the defined joint connection between members of the 5th bay which is assumed pinned and modeled as a rotational joint. The Elements used in the analysis are BEAM 189 for all beam members and MPC 184 for the joint connections between beams and columns. Two different nonlinear materials with different yield strength are defined and are attributed to beams and columns respectively.

3.2.4 Dynamic Properties

The seismic demands of the building will be computed by nonlinear static analysis subjected to monotonically increasing lateral forces with an invariant height-wise distribution. In the modal pushover analysis method a pushover analysis is performed for each mode separately with the following force distribution:

$$s_n^* = m\phi_n \tag{3.4}$$

In order to obtain a modal distribution of forces, a 2D modal analysis is performed. A point mass is attributed at each story level, equal to half of the story weight, see figure 3.13. The material used for the steel is isotropic elastic. The whole frame is attributed a displacement boundary condition equal to $z = 0$, so that the structure is detained from deflecting out of the plane.

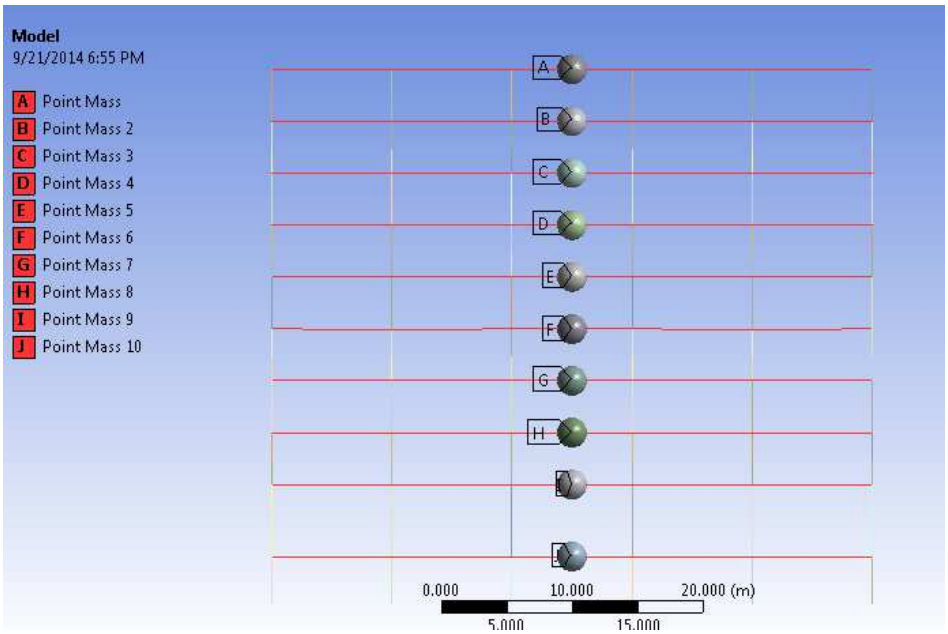

FIGURE 3.13: Modal analysis with point mass.

LEVEL	MODE 1	MODE 2	MODE 3
1	0.18	-0.49	0.96
2	0.28	-0.71	1.20
3	0.41	-0.84	0.86
4	0.55	-0.84	-0.06
5	0.68	-0.68	-0.76
6	0.78	-0.38	-1.15
7	0.87	0.07	-0.88
8	0.95	0.59	0.00
9	1.00	1.00	1.00

TABLE 3.2: Mode shapes for the 9 story building.

In Figures 3.15 3.16 and 3.17 the first three natural modes of vibration obtained in ANSYS are presented and Figure 3.14 is a graphic in Excel displaying the normalized three modes.This values will be introduced in the formula 3.4 in order to obtain the

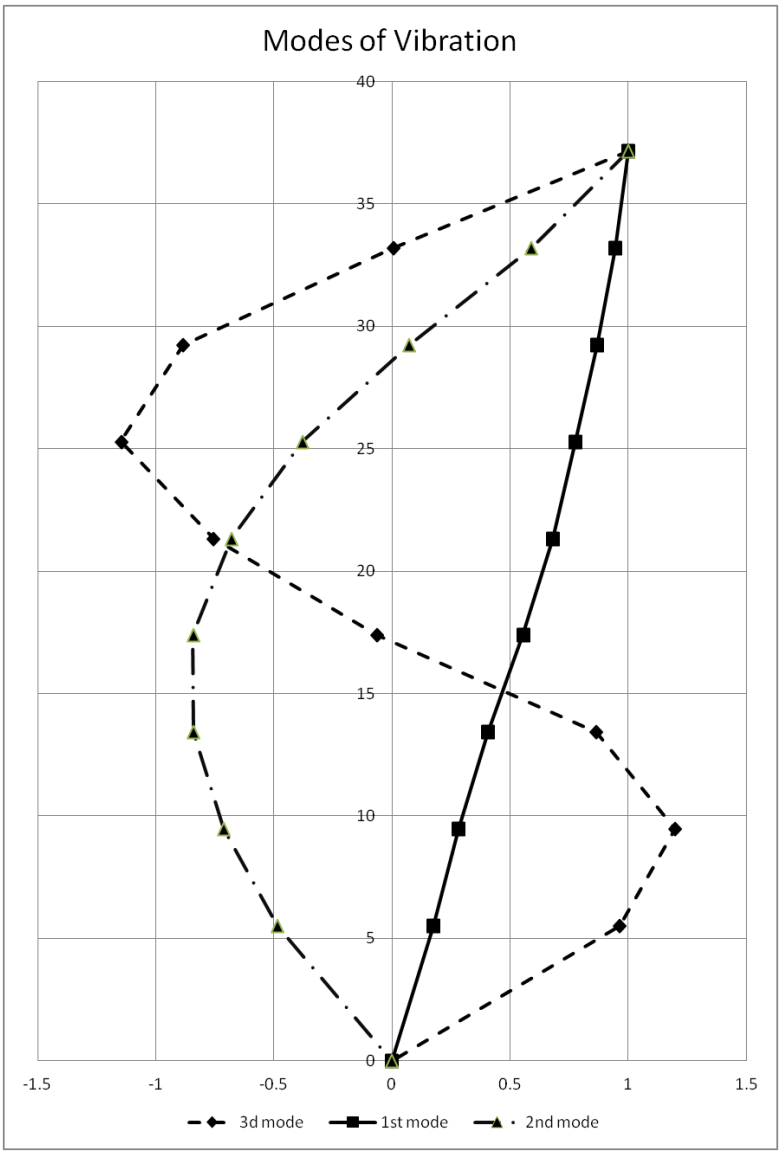

FIGURE 3.14: Normalized natural modes of vibration.

MODE	FREQUENCY	PERIOD	PARTICIPATION FACTOR
1	0.441	2.268	-2067.3
2	1.261	0.792	732.16
3	2.054	0.486	450.86

TABLE 3.3: Dynamic properties: natural frequencies, periods, participation factor.

MODE	RATIO	EFFECTIVE MASS	CUMULATIVE MASS FRAC-TION	RATIO EFF. M TO TO-TAL M
1	1.000000	0.427E+07	0.852524	0.753
2	0.354155	536055.	0.959452	0.095
3	0.218088	203275.	1.00000	0.036

TABLE 3.4: Dynamic properties: ratio, effective mass, cumulative mass fraction, ratio effective mass to total mass.

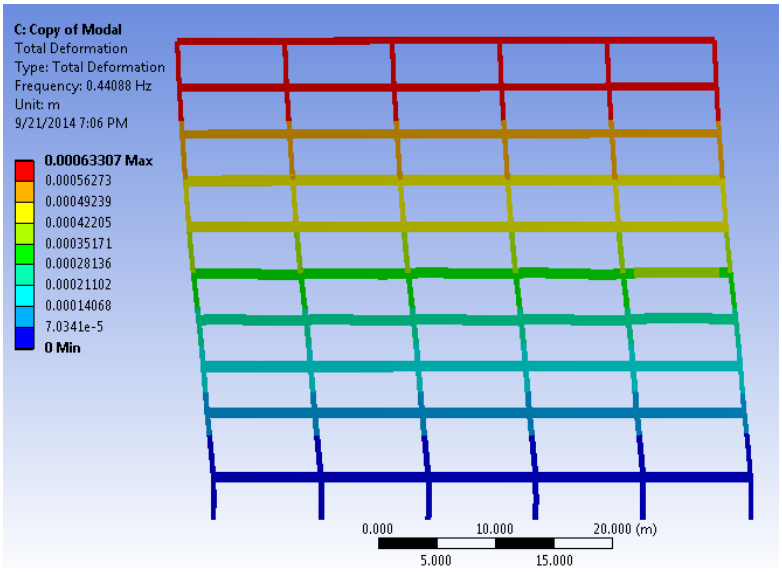

FIGURE 3.15: Mode 1.

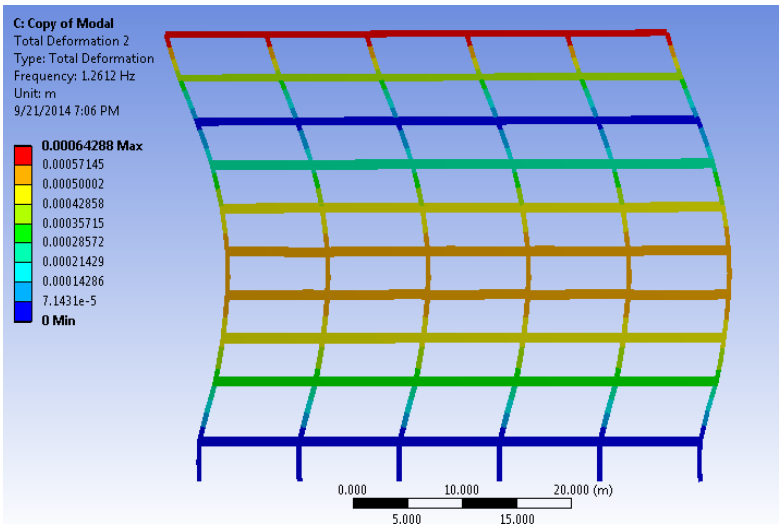

FIGURE 3.16: Mode 2.

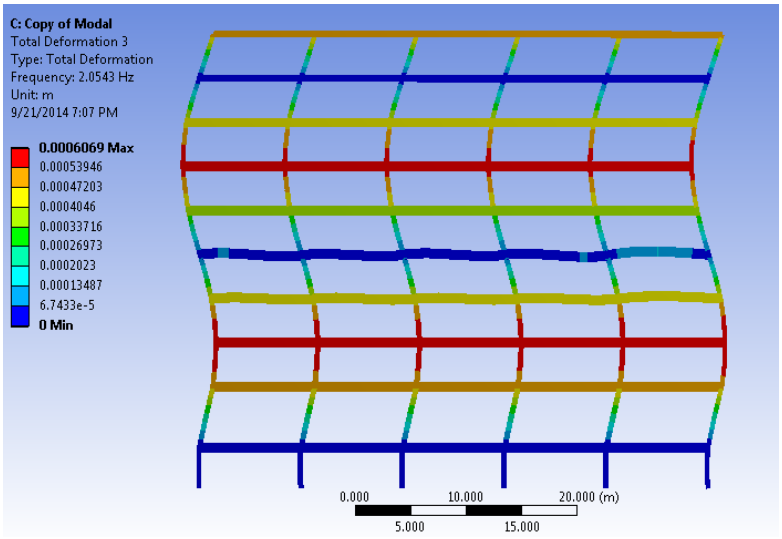

FIGURE 3.17: Mode 3.

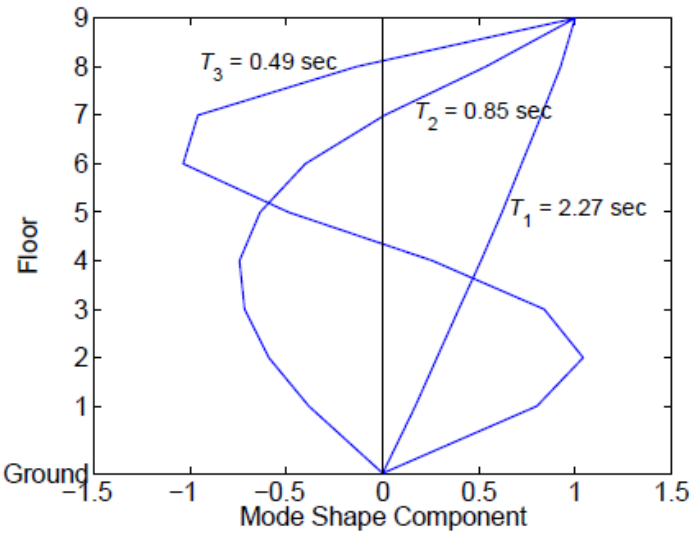

FIGURE 3.18: Modes from paper [6].

lateral forces for the three pushover curves. The dynamic properties are compared to the ones provided in the paper mentioned as reference literature [6] and which are displayed in Figure 3.18. The values of the vibration periods for the first three modes are 2.27, 0.85 and 0.49 s, respectively, and are in good accordance with the ones obtained with ANSYS, see the values in table 3.3 so the analysis moves on to the next step.

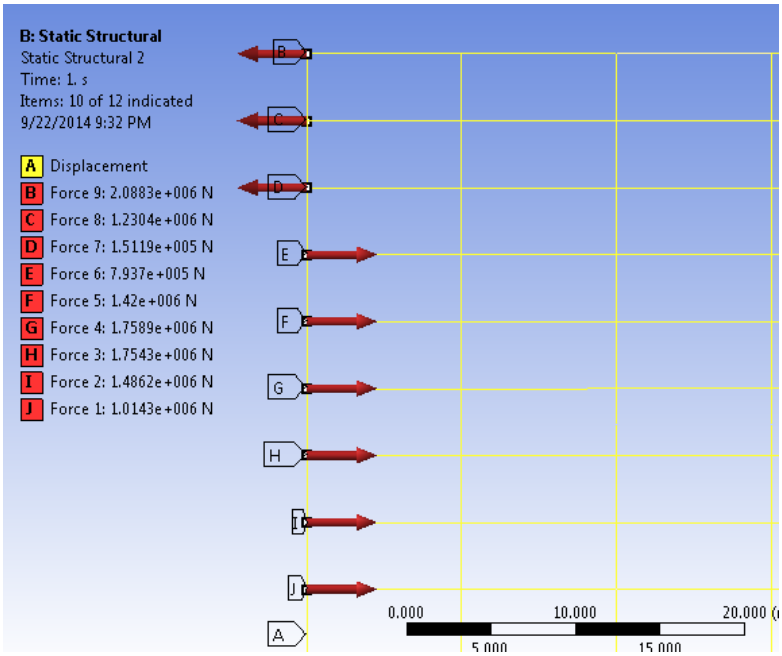

FIGURE 3.19: Distribution of forces.

3.2.5 The Pushover Analysis

For the n-th mode, the base shear-roof displacement, $V_{bn} - r_{rn}$, pushover curve for the force distribution 3.4 is developed. In ANSYS the displacements linked to the modal analysis are parametized, multiplied with the mass of each storey and introduced in the new analysis as lateral forces, see Figure 3.19 as an example fo the applied forces for force distribution of mode 2.

In the next step, the pushover curve is idealized as a bilinear curve. If the pushover curve exhibits negative post-yielding stiffness, the pushover curve is idealized as elastic-perfectly-plastic. The gravity loads were not included in the analysis, so the curve does not exhibit negative post-yielding stiffness. The pushover curve is idealized by mantaining the initial stiffness slope and determining the tangent stiffness by setting the area below the pushover curve equal to the one below the idealized bilinear curve. This leads to the location of the yielding point for the idealized curve, defined by the yielding Force F_{sny} and deformation D_{ny}.

The pushover curves are potted in the following figures, together with the idealized curve, first as a Base Shear V_b in kN - roof displacement u_t in cm relationship. The

second plot is a base shear/ total weight of the building - roof displacement/ total height relationship.

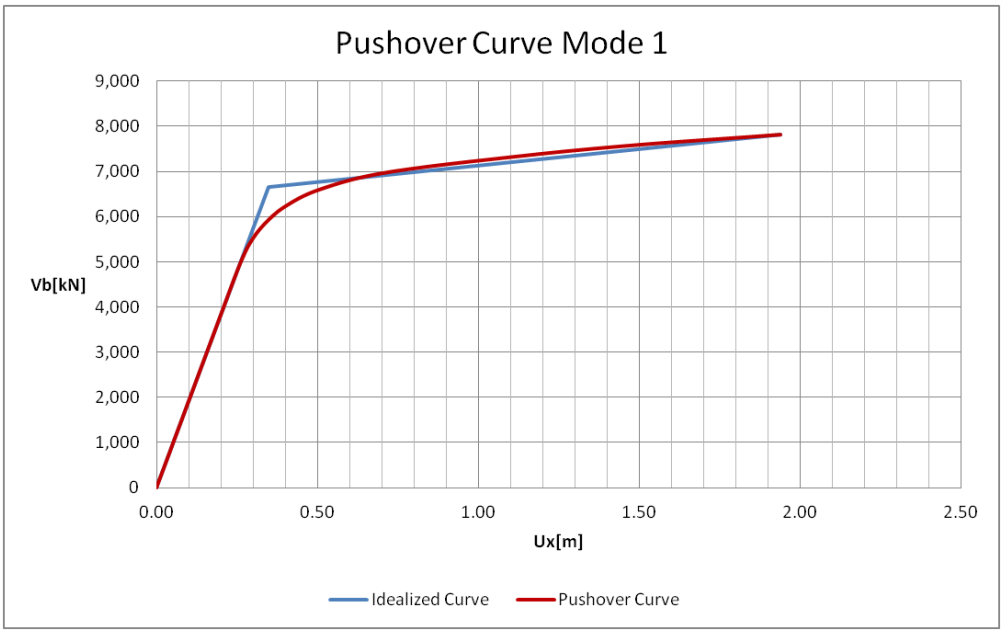

FIGURE 3.20: Pushover curve for the first modal distribution of forces.

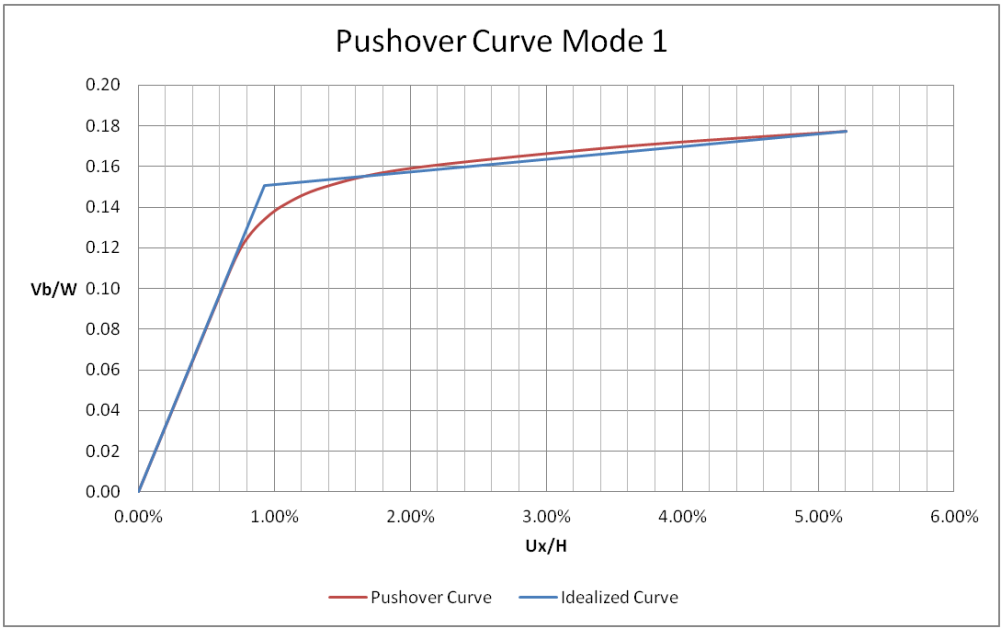

FIGURE 3.21: Pushover curve for the first modal distribution of forces.

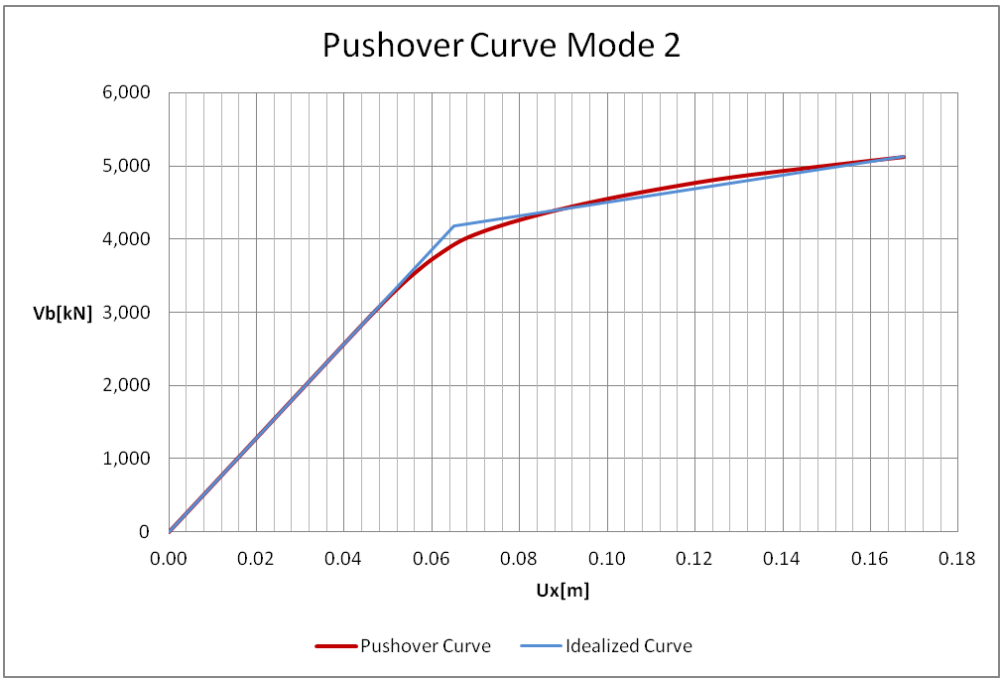

FIGURE 3.22: Pushover curve for the second modal distribution of forces.

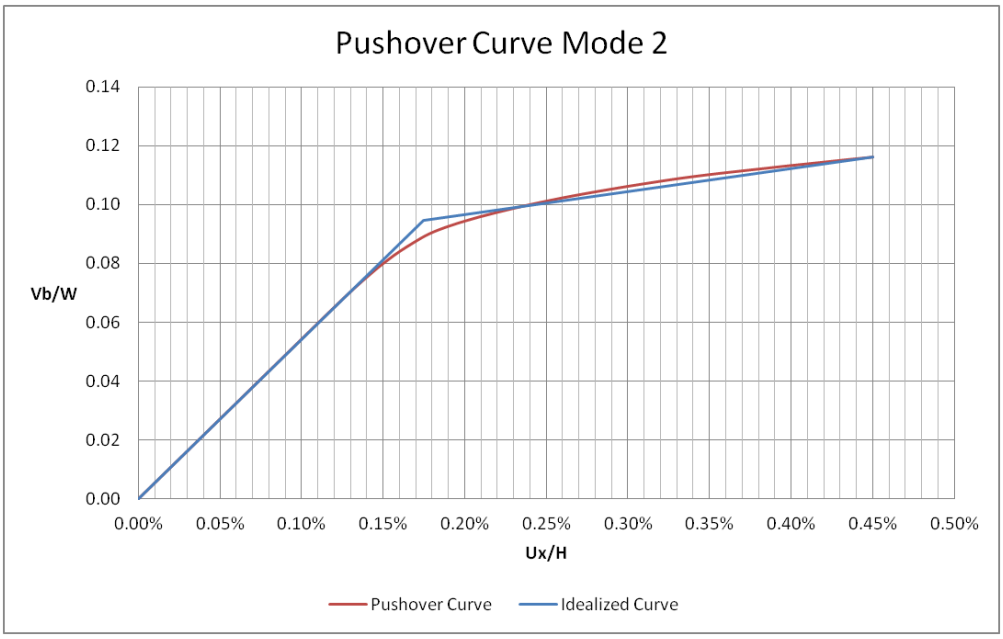

FIGURE 3.23: Pushover curve for the second modal distribution of forces.

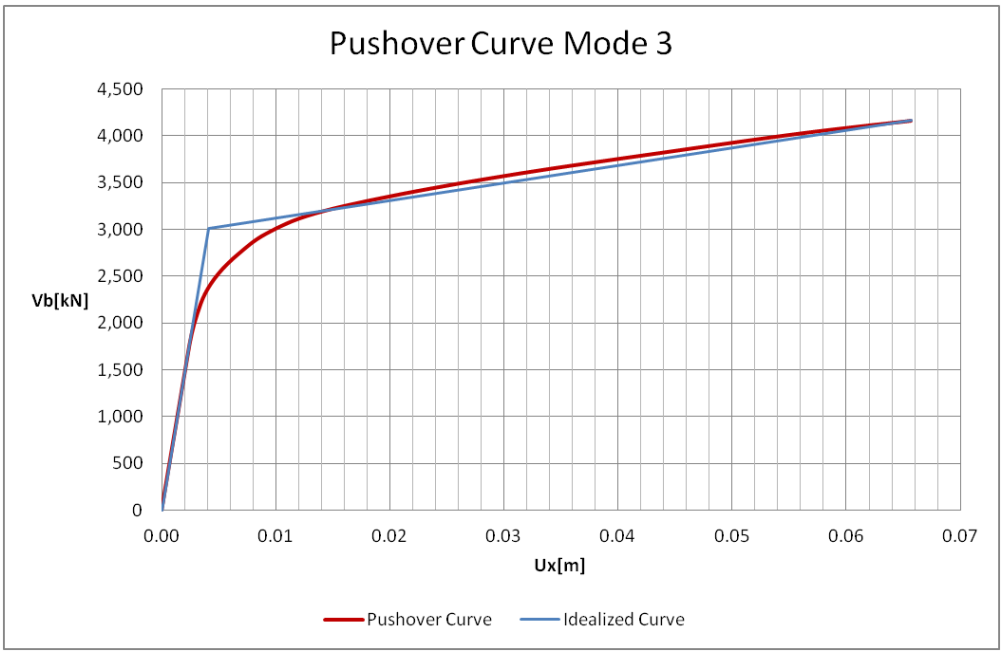

FIGURE 3.24: Pushover curve for the third modal distribution of forces.

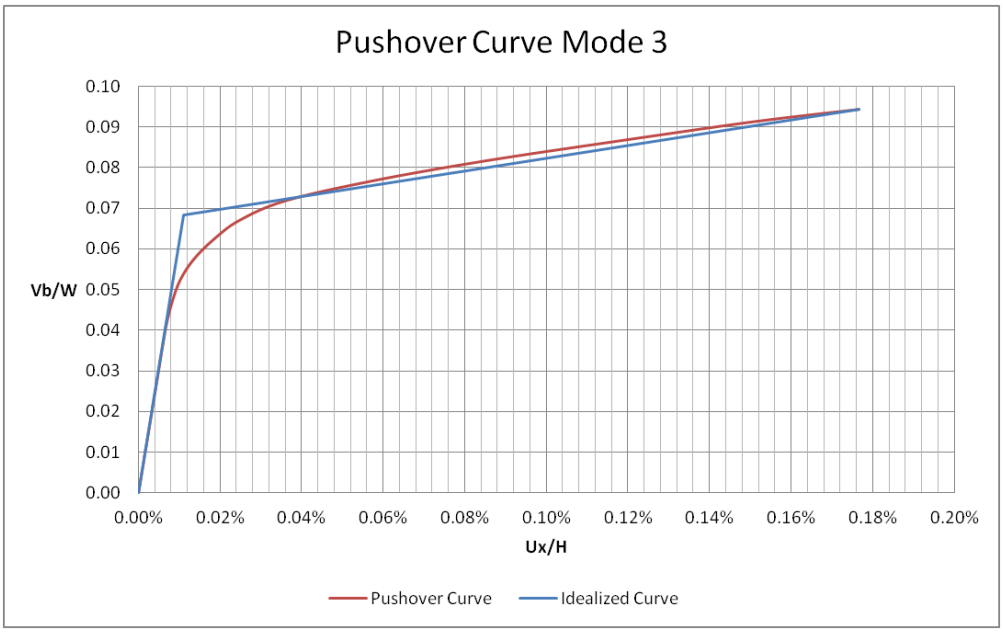

FIGURE 3.25: Pushover curve for the third modal distribution of forces.

3.2.6 Target Displacement

Once the idealized pushover curve is determined, it is converted to the force displacement relation $F_{sn}/L_n - D_n$, in order to compute the peak deformation D_n of the nth mode inelastic SDF system. This system is defined by the force deformation relation, by its damping ratio ζ_n and by the elastic vibration period of the system T_n, see equation 1.38. D_n can be computed by nonlinear response history analysis or from the inelastic design spectrum. The peak deformation D_n is then used to calculate the peak roof displacement u_{rn}, as in equation 1.39. In order to render results comparable to the ones available in the study [7], the peak roof displacement is determined through nonlinear RHA of the building subjected to 1.5 x the El Centro ground motion. The values of peak roof displacement are determined for each mode separately. The governing equation of the nth mode inelastic SDF system is:

$$\ddot{D}_n + 2\zeta_n\omega_n\dot{D}_n + \frac{F_{sn}}{L_n} = -\ddot{u_g}t \tag{3.5}$$

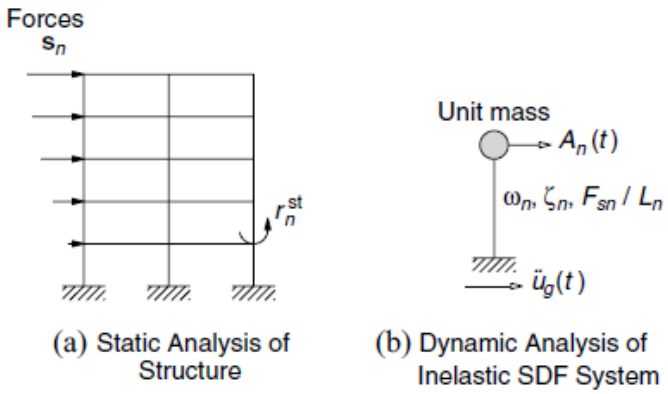

FIGURE 3.26: Conceptual explanation of uncoupled modal RHA of inelastic MDF systems. [7]

The values of the roof displacements determined by RHA of the nth-mode inelastic SDF system are $u_{rn0} = 48.3$, 11.7 and $2.53cm$ respectively, see Figure concept. The conceptual explanation of the procedure is shown in Figure 3.27. These values are extracted from the study [7] in order to render comparable results. They are further applied in the present study and are implemented as the unknown target displacements. Thus, the structure is pushed for each modal distribution of forces to each of these target displacements respectively, see Figure 3.28. At this point the desired values are

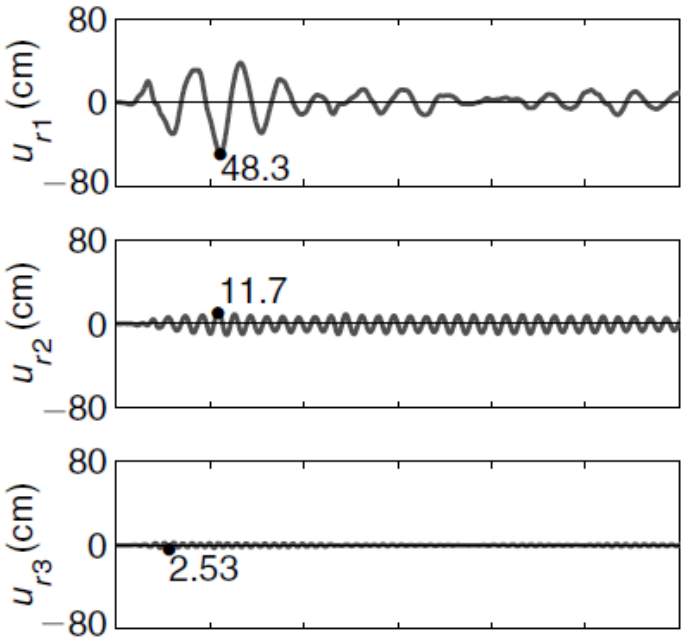

FIGURE 3.27: Response histories of roof displacement and top-storey drift due to 1.5 × El Centro ground motion: individual 'modal' responses. [7]

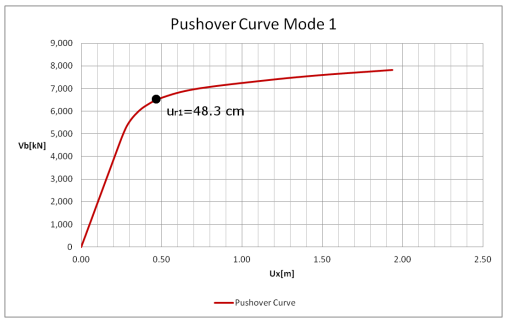

(A) Target displacement for mode 1.

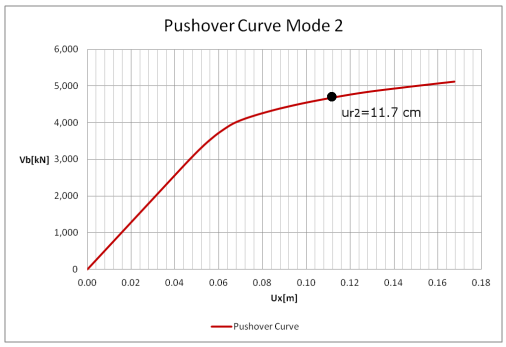

(B) Target displacement for mode 2.

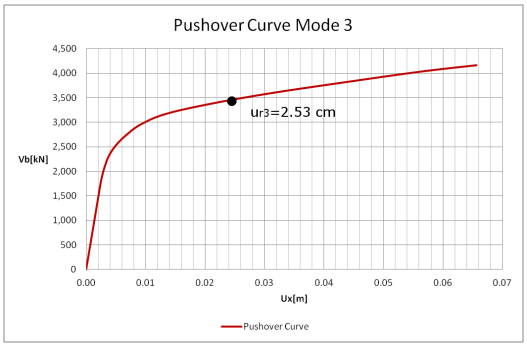

(C) Target displacement for mode 3.

FIGURE 3.28: Modal pushover curves with peak roof displacements for 1.5 x El Centro ground motion.

extracted from the pushover data base from ANSYS: floor displacements, story drifts and plastic hinge locations.

Chapter 4

Results and Comparison

4.1 Pushover Curve - Comparison

	Present Study		Chopra and Goel	
Mode	Yield Strength V_{by}/W	Yield Displacement u_y [cm]	Yield Strength V_{by}/W	Yield Displacement u_y[cm]
1	0.1551	34.6	0.1684	36.3
2	0.0947	7.1	0.1122	9.9
3	0.0683	1.2	0.1181	4.6

TABLE 4.1: Yield strength and yield displacement of the idealized pushover curve for the first three modes of vibration - current study vs. literature.

Mode	Yield Strength V_{by}/W	Yield Displacement u_y
1	7.90	4.68
2	15.60	28.28
3	42.17	73.91

TABLE 4.2: Difference in percentage between the two studies.

In this section the results of the study are presented together with the ones from Literature [7], [6], [8] and [5] for comparison. The three pushover curves were plotted in the previous chapter. Table 4.1 shows the yield strength and displacement of the idealized pushover curve. As can be seen in table 4.2, the two sudies yield similar results for the first mode, yet for the second and, most obvious, for the third mode they are very different. Figure 4.1 shows the results from the study [7] . For mode number 3, what

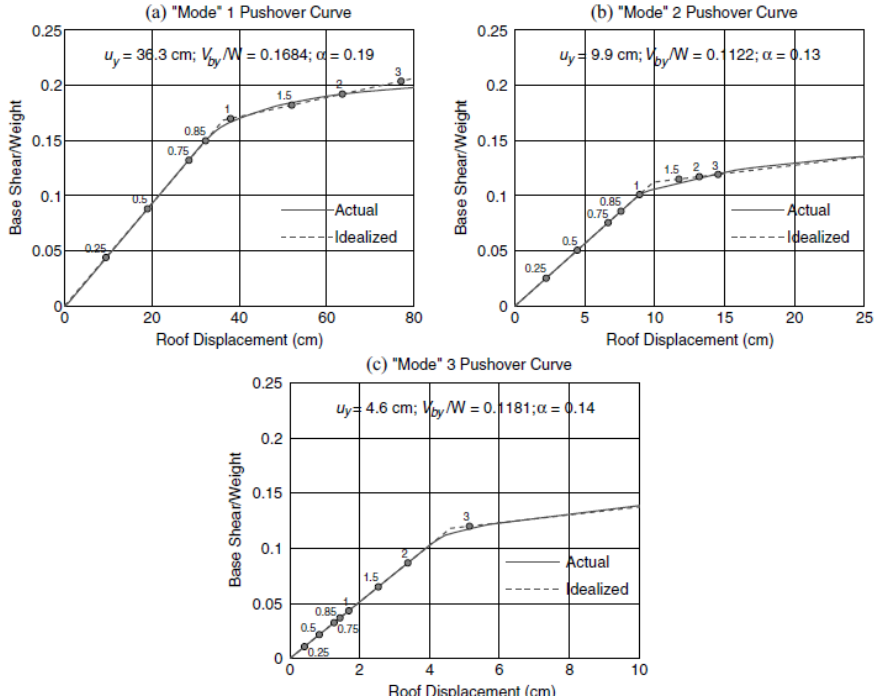

FIGURE 4.1: Modal pushover curves from the study [8] with peak roof displacements identified for the El Centro ground motion.

can be seen in comparison with Figure 3.28, what can be seen is that in the current study the 1.5 X El Centro ground motion leads to yielding of the structure.

4.2 Story Drifts and Displacements

In this section the height- wise variation of floor displacements and story drift ratios from MPA for the 1.5 X El Centro ground motion are presented. The values are extracted from ANSYS for every mode at the respective target displacement. The definition of story is:

$$\Delta_n = u_n - u_{n-1} \tag{4.1}$$

where u_n is the floor displacement of story n.

The definition of story drift ratio is:

$$\delta_n = \frac{\Delta_n - \Delta_{n-1}}{h_n} \tag{4.2}$$

where n is the story number, h_n the stroy height and Δ_n the story drift.

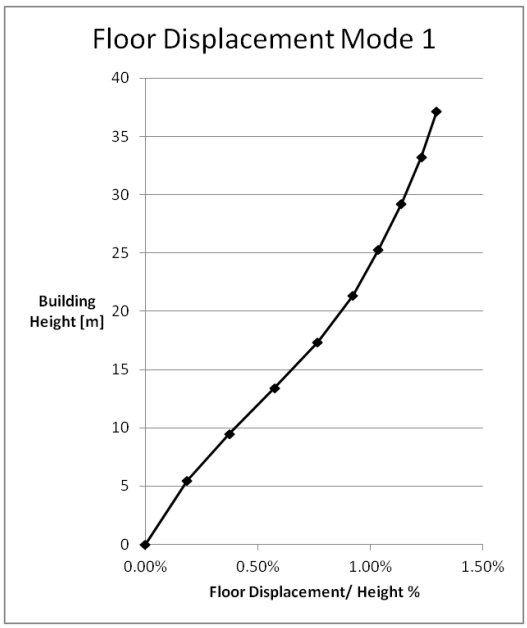

(A) Floor displacements for the first mode pushover curve.

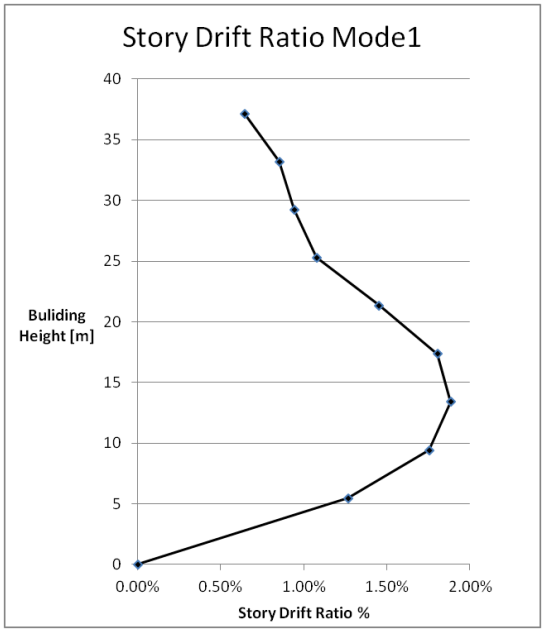

(B) Story drift ratio for the first mode pushover curve.

FIGURE 4.2: Values from ANSYS at target displacement ur1.

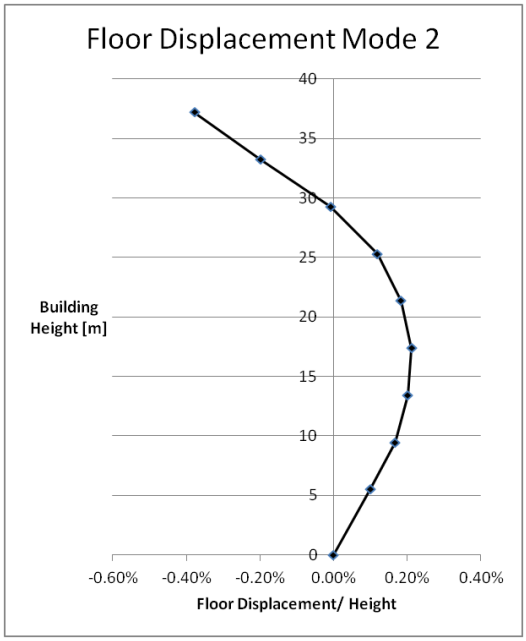

(A) Floor displacements for the second mode pushover curve.

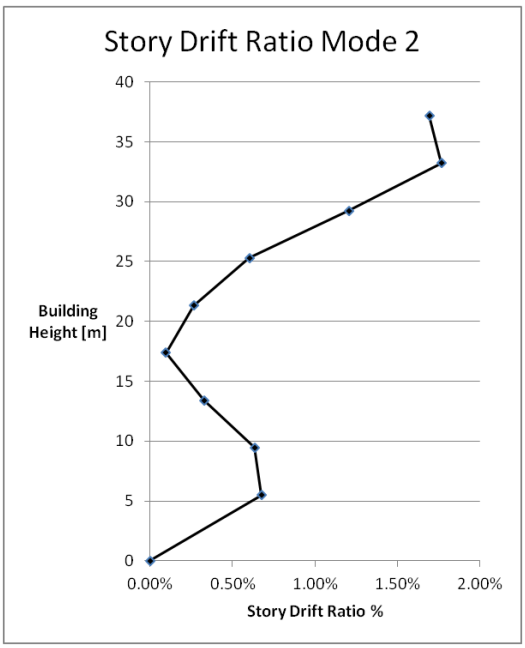

(B) Story drift ratio for the second mode pushover curve.

FIGURE 4.3: Values from ANSYS at target displacement ur2.

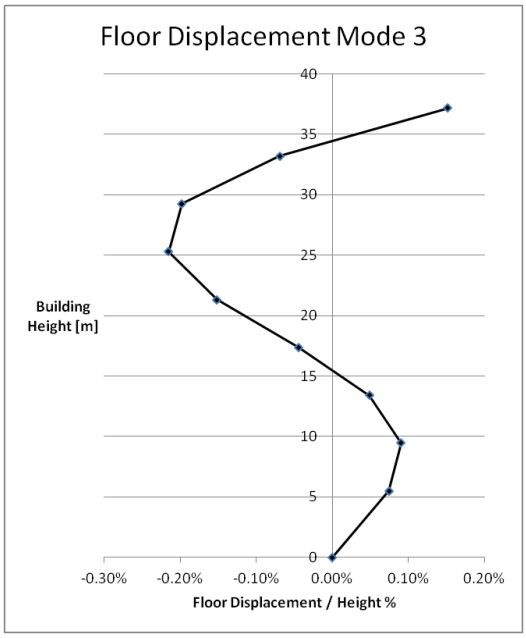

(A) Floor displacements for the third mode pushover curve.

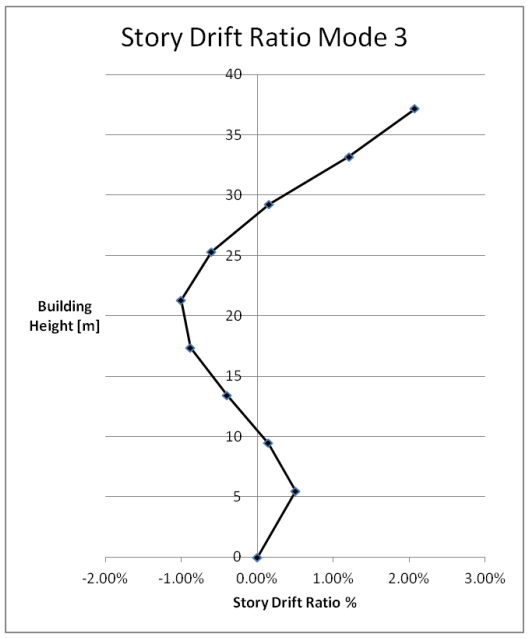

(B) Story drift ratio for the third mode pushover curve.

FIGURE 4.4: Values from ANSYS at target displacement ur3.

Using The SRSS combination rule, the three sets of values from the three modes of vibration are combined and then plotted.

For comparison the floor displacements and story drifts for the first three modes of vibration, as well as the results from RHA, presented in the paper [7], see Figure 4.7.

It can be observed that the combined first two modes of vibration yield a result wich is in good accordance with the RHA. However. the result from ANSYS for the third mode of vibration seem to overestimate the story drifts and displacements, if compared to the solution with RHA. [5]

4.3 Location of Plastic Hinges

Following, the location of Plastic Hinges for the three modes of vibration are presented:

For comparison, the location of plastic hinges in the paper [7], together with the plastic hinge location by performing a RHA:

In the paper [7], the pushover analysis fails to predict the plastic hinge formation at the ground floor columns, which the present study predicts. However the whole system

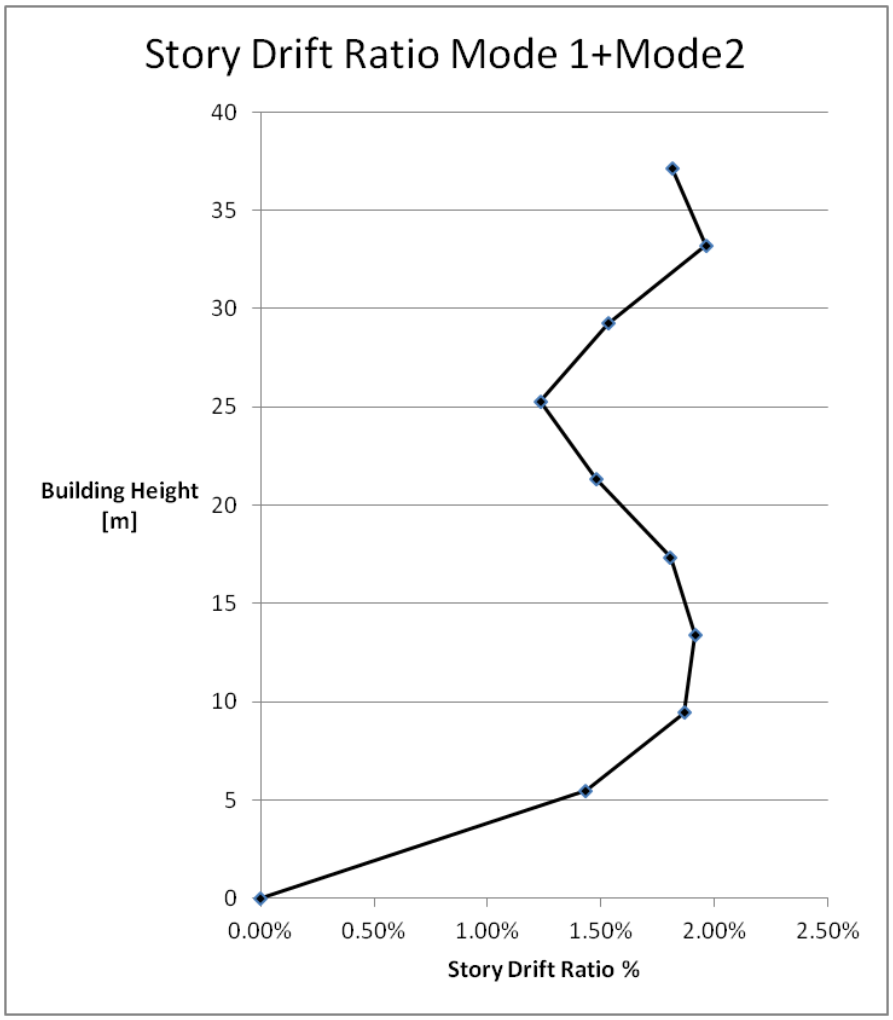

FIGURE 4.5: Story drift ratio for the combined first two modes pushover curve.

seems to be not as rigid and a few more plastic hinges appear. This is also due to the fact that the pushover analysis for the third mode of vibration also leads to formation of plastic hinges, especially in the upper floors.

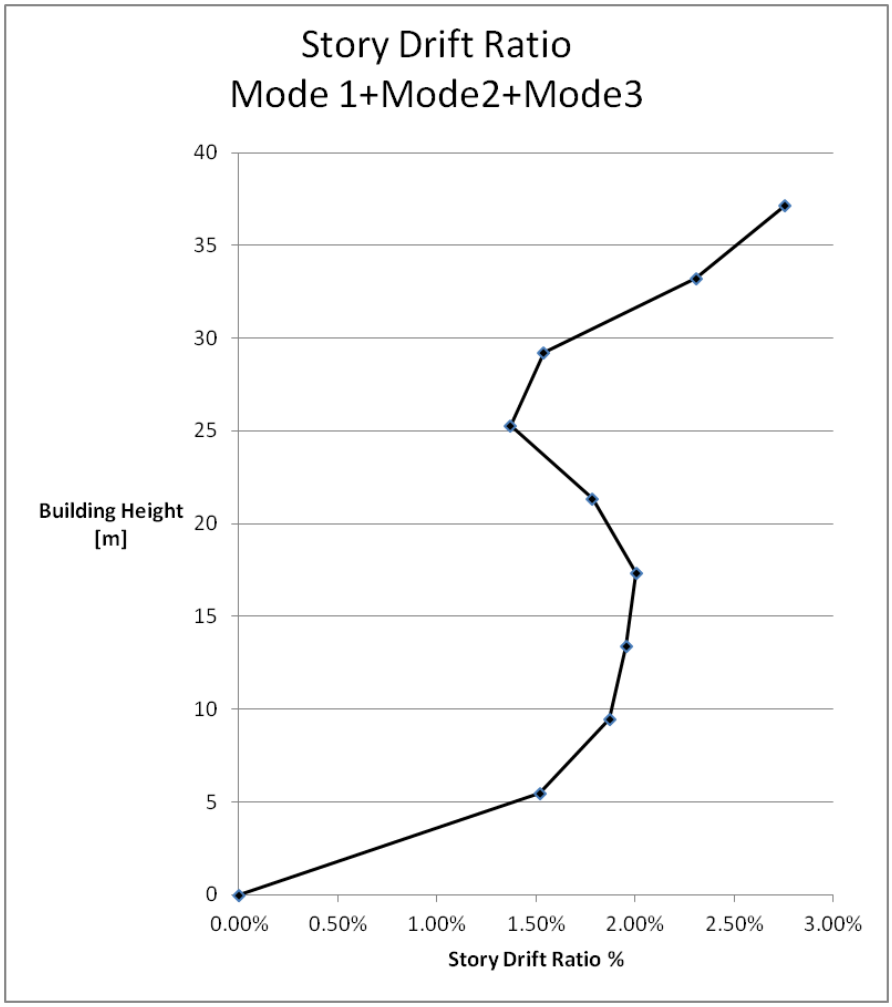

FIGURE 4.6: Story drift ratio for the combined first three modes pushover curve.

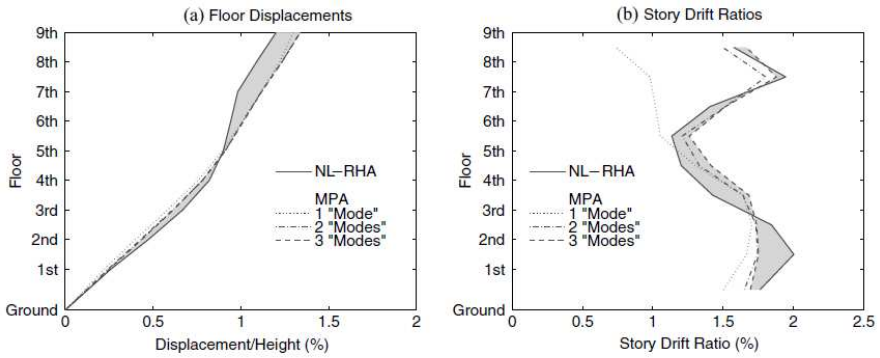

FIGURE 4.7: Results from literature [7].

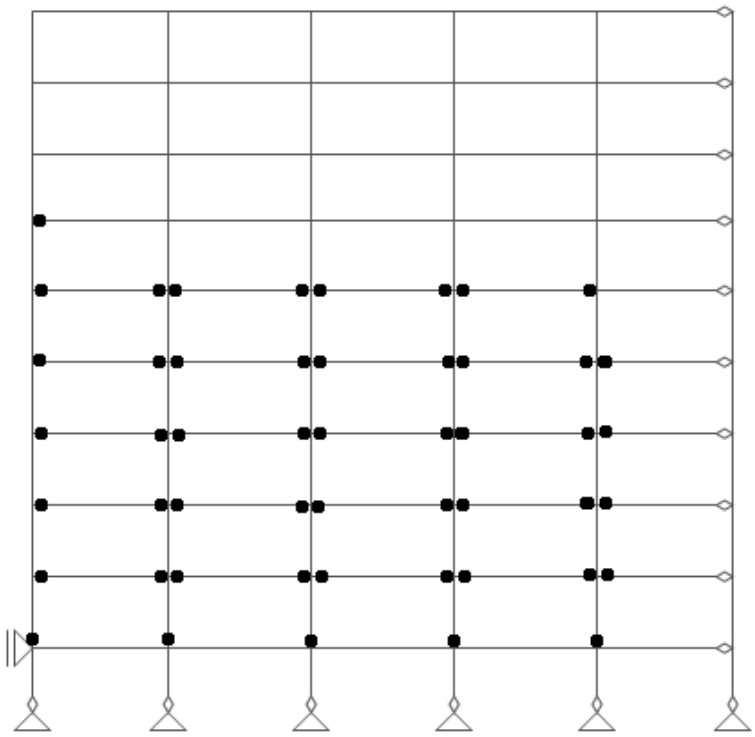

FIGURE 4.8: Plastic hinge location for the first mode pushover curve.

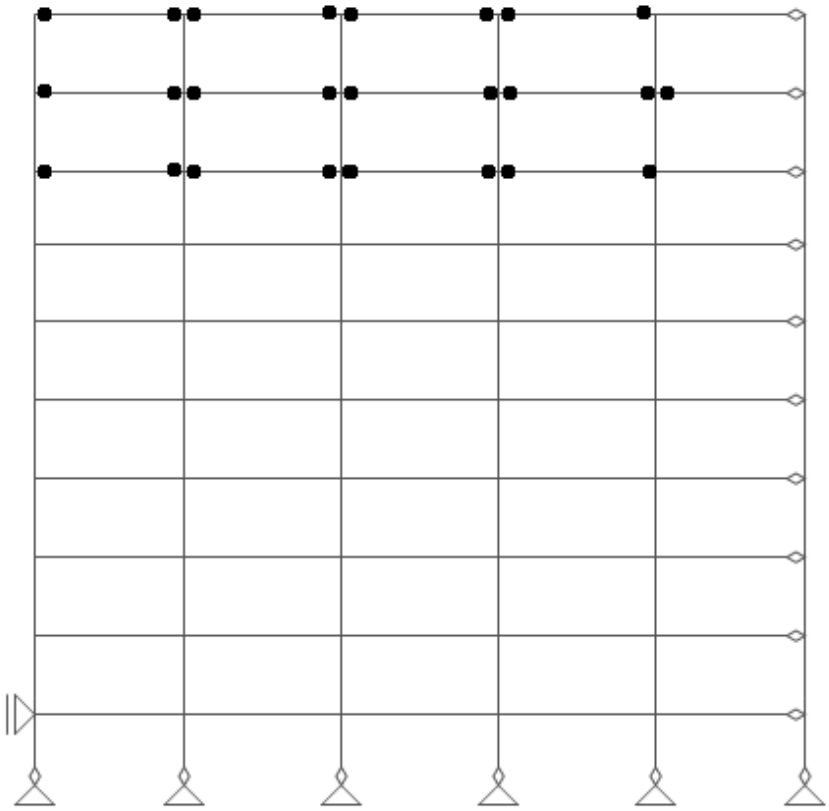

FIGURE 4.9: Plastic hinge location for the second mode pushover curve.

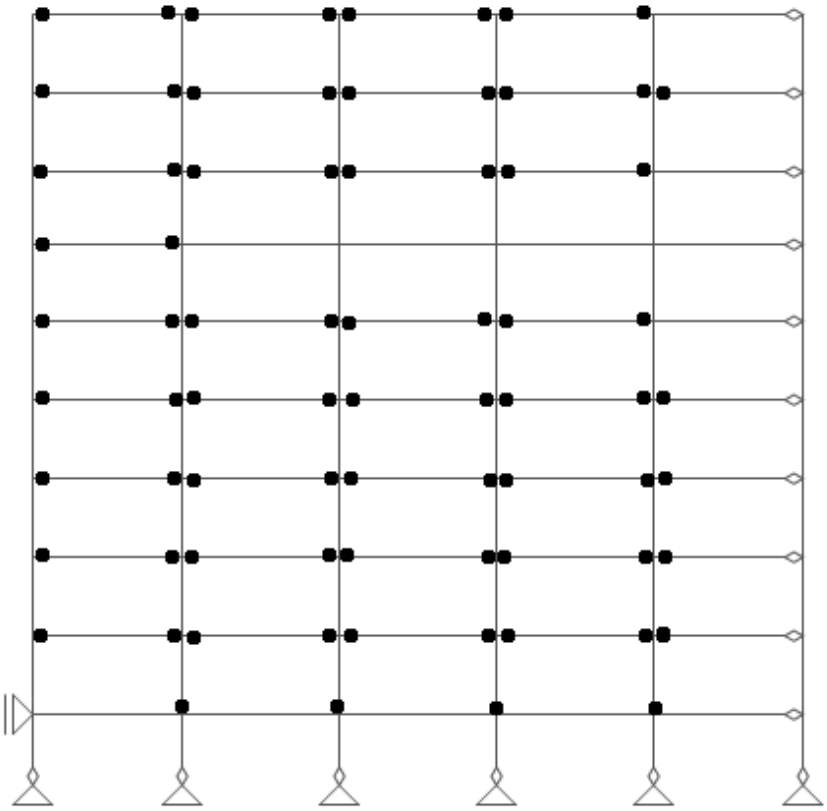

FIGURE 4.10: Plastic hinge location for the combined first three modes pushover curve.

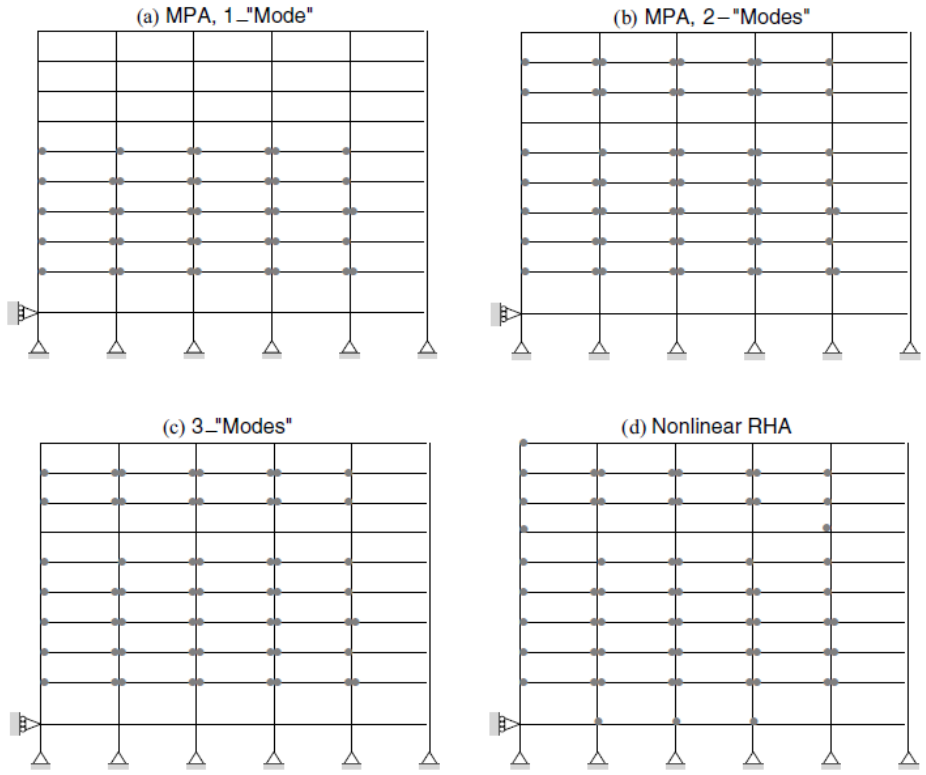

FIGURE 4.11: Plastic hinge location in the paper [7].

Chapter 5

Conclusion

The MPA procedure for an inelastic system is structured as follows: first the dynamic properties of the system are computed and a pushover curve is determined using the inertia force distribution of each mode separately. In a further step, the target displacement is evaluated by RHA and the values of the desired results are extracted from the pushover data base: floor displacements, story drifts, plastic hinge locations. The total response is obtained by combining those results using the SRSS rule.

The results are in good accordance with the RHA if compared for the first two modes of vibration. The combined results lead to very similar demands for the floor displacements and story drifts. In comparison with the study ??, it also determines the location of plastic hinges more accurately, for example by predicting the plastic hinge formation in the column base of the ground floor. However the results from the third mode of vibration were less accurate, overestimating the actual story drifts.

ANSYS can be described as a very powerful tool for analyzing nonlinear systems, with various capabilities to model the actual building. As has been described in chapter 2, the nonlinear system can be specified through various parameters: material and geometric nonlinearity as well as nonlinear connections between members. The problem will eventually become very complex and the question may arise if so much accuracy is actually needed in order to assess the seismic demand by pushover analysis, which is itself based on various assumptions. As for the modal pushover analysis, it can easily be implemented in ANSYS, by performing a modal analysis of the system prior to adjusting it in order to perform the static pushover analysis.

Bibliography

[1] Gregory G. Deierlein, Andrei M. Reinhorn, and Michael R. Willford. Nonlinear structural analysis for seismic design. *NEHRP Seismic Design Technical Brief*, 4, 2010. URL `http://www.nehrp.gov/pdf/nistgcr10-917-5.pdf`.

[2] American Society of Civil Engineers. Seismic rehabilitation of existing buildings. American society of civil engineers, 2007.

[3] Miodrag Sekulovic, Ratko Salatic, and Marija Nefovska. Dynamic analysis of steel frames with flexible connections. *Computers & structures*, 80(11):935–955, 2002.

[4] Peter Kohnke. Ansys theory manual. *ANSYS Inc*, 178, 2001.

[5] Akshay Gupta and Helmut Krawinkler. *Seismic demands for the performance evaluation of steel moment resisting frame structures*. PhD thesis, Stanford University, 1999.

[6] Rakesh K Goel and Anil K Chopra. Evaluation of modal and fema pushover analyses: Sac buildings. *Earthquake Spectra*, 20(1):225–254, 2004.

[7] Anil K Chopra and Rakesh K Goel. A modal pushover analysis procedure for estimating seismic demands for buildings. *Earthquake Engineering & Structural Dynamics*, 31(3):561–582, 2002.

[8] Anil K Chopra and Rakesh K Goel. A modal pushover analysis procedure to estimate seismic demands for unsymmetric-plan buildings: theory and preliminary evaluation. *Earthquake Engineering Research Center*, 2003.

[9] Ronald O. Hamburger. A framework for performance-based earthquake resistive design. *National Information Service for Earthquake Engineering*, 1997. URL `http://nisee.berkeley.edu/lessons/hamburger.html`.

[10] Comité Européen de Normalisation. Eurocode 8–design of structures for earthquake resistance–part 1: General rules, seismic actions and rules for buildings. *European Standard NF EN*, 1, 1998.

[11] Building Seismic Safety Council (US) and Applied Technology Council. *NEHRP guidelines for the seismic rehabilitation of buildings*, volume 1. Federal Emergency Management Agency, 1997.

[12] Anil K. Chopra and Rakesh K. Goel. Response to b. maison's discussion of "evaluation of modal and fema pushover analysis: Sac buildings". *Earthquake Spectra*, (21).

[13] H. Krawinkler and G. D. P. K. Seneviratna. Pros and cons of a pushover analysis of seismic performance evaluation. *Engineering Structures*, 20(4-6):452–464, 1998. URL `http://imacwww.epfl.ch/genieparasismique/edoc_st09/course_3/krawinkler_sene_98.pdf`.

[14] JY Richard Liew, DW White, and Wai-Fah Chen. Second-order refined plastic-hinge analysis for frame design. part i. *Journal of Structural Engineering*, 119(11): 3196–3216, 1993.

[15] M. A. Crisfield. *Non-linear Finite Element Analysis of Solids and Structures*, volume 1. John Wiley Sons Ltd., 1991.

[16] Marianne Swanson, Nadya Bartol, Rama Moorthy, et al. Analysis systems. In *ANSYS Theoretical Manual*. Citeseer, 1991.

[17] E Hinton. *Introduction to Nonlinear Finite Element Analysis.s*. NAFEMS, 1992.

9 Story Building

COLUMNS	AREA[m²]	d[cm]	tw[cm]	bf[cm]	tf[cm]
W14X233	0.04419	40.7	2.7	40.4	4.4
W14X257	0.04877	41.6	3	40.6	4.8
W14X283	0.05374	42.5	3.3	40.9	5.3
W14X370	0.07032	45.5	4.2	41.8	6.8
W14X455	0.08645	48.3	5.1	42.8	8.2
W14X500	0.09484	49.8	5.6	43.2	8.9
BEAMS	AREA[m²]	d[cm]	tw[cm]	bf[cm]	tf[cm]
W24X68	0.01297	60.3	1.1	22.8	1.5
W27X84	0.01600	67.8	1.2	25.3	1.6
W30X99	0.01877	75.3	1.3	26.5	1.7
W36X135	0.02561	90.3	1.5	30.4	2
W36X160	0.03032	91.5	1.7	30.5	2.6

TABLE 1: Cross section dimensions of the MRF.

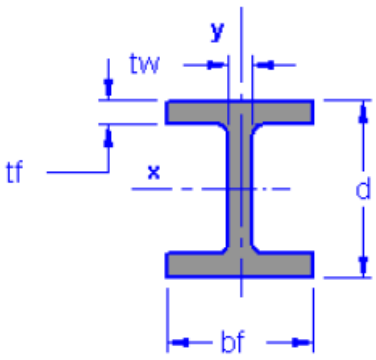

FIGURE 1: Cross section parameters.

COLUMNS	Ixx[in^4]	Iyy[in^4]	Ixx[cm^4]	Iyy[cm^4]
W14X233	3010	1150	125286	47867
W14X257	3400	1290	141519	53694
W14X283	3840	1440	159833	59937
W14X370	5440	1990	226430	82830
W14X455	7190	2560	299270	106555
W14X500	8210	2880	341726	119875
BEAMS	Ixx[in^4]	Iyy[in^4]	Ixx[cm^4]	Iyy[cm^4]
W24X68	1830	70.4	76170	2930
W27X84	2850	106	118626	4412
W30X99	3990	128	166076	5328
W36X135	7800	225	324660	9365
W36X160	9750	295	405826	12279

TABLE 2: Cross section moments of inertia in [in^4] and [cm^4] of the MRF.

	Mass for both MRFs [kg]	Mass for one Frame [kg]
Ground Floor	965000	482500
1st Floor	1010000	505000
2nd-8th Floor	989000	494500
9th Floor	1070000	535000
Mass of above ground levels	8979000	

TABLE 3: Seismic mass of the structure including steel framing for N-S MRFs.